Michigan Technological University

UNDERGRADUATE RESEARCH SYMPOSIUM 2017

Welcome to the 2017 Undergraduate Research Symposium!

The Undergraduate Research Symposium highlights the amazing cutting-edge research being conducted on Michigan Tech's campus by some of our best and brightest undergraduate students.

The students showcasing their work today have spent a significant portion of the past year working alongside Michigan Tech faculty and graduate students to explore, discover and create new knowledge. They've spent long hours in the lab or out in the field designing experiments, gathering data, creating new models and testing hypotheses. They've applied their classroom knowledge in new and sometimes unexpected ways, and developed new skills that will propel them forward in their careers.

Each of the presenters has been mentored by a faculty member who took great care to guide them through the rigors and exhilaration of pioneering research projects. They've shared in arduous tasks, brainstormed, adjusted hypotheses and regrouped as their projects have taken shape. Through the process, they've built strong relationships that will last a lifetime. The students presenting today represent a wide array of disciplines from across campus and highlight the diversity of research areas being explored.

I would like to take this opportunity to thank our partners and sponsors who have funded the work of many of the students that you will see on display today. In particular, I want to recognize the office of the Vice President for Research for funding the Summer Undergraduate Research Fellowship Program, as well as the Portage Health Foundation, the DeVlieg Foundation, and the Michigan Space Grant Consortium for funding the Undergraduate Research Internship Program.

I sincerely hope that you enjoy visiting with our students and learning about their research endeavors today. Challenge them with your questions and experience the passion that is Michigan Tech!

Sincerely,

Lorelle Meadows
Dean, Pavlis Honors College

Pavlis Honors College

Michigan Tech

Undergraduate Research Symposium

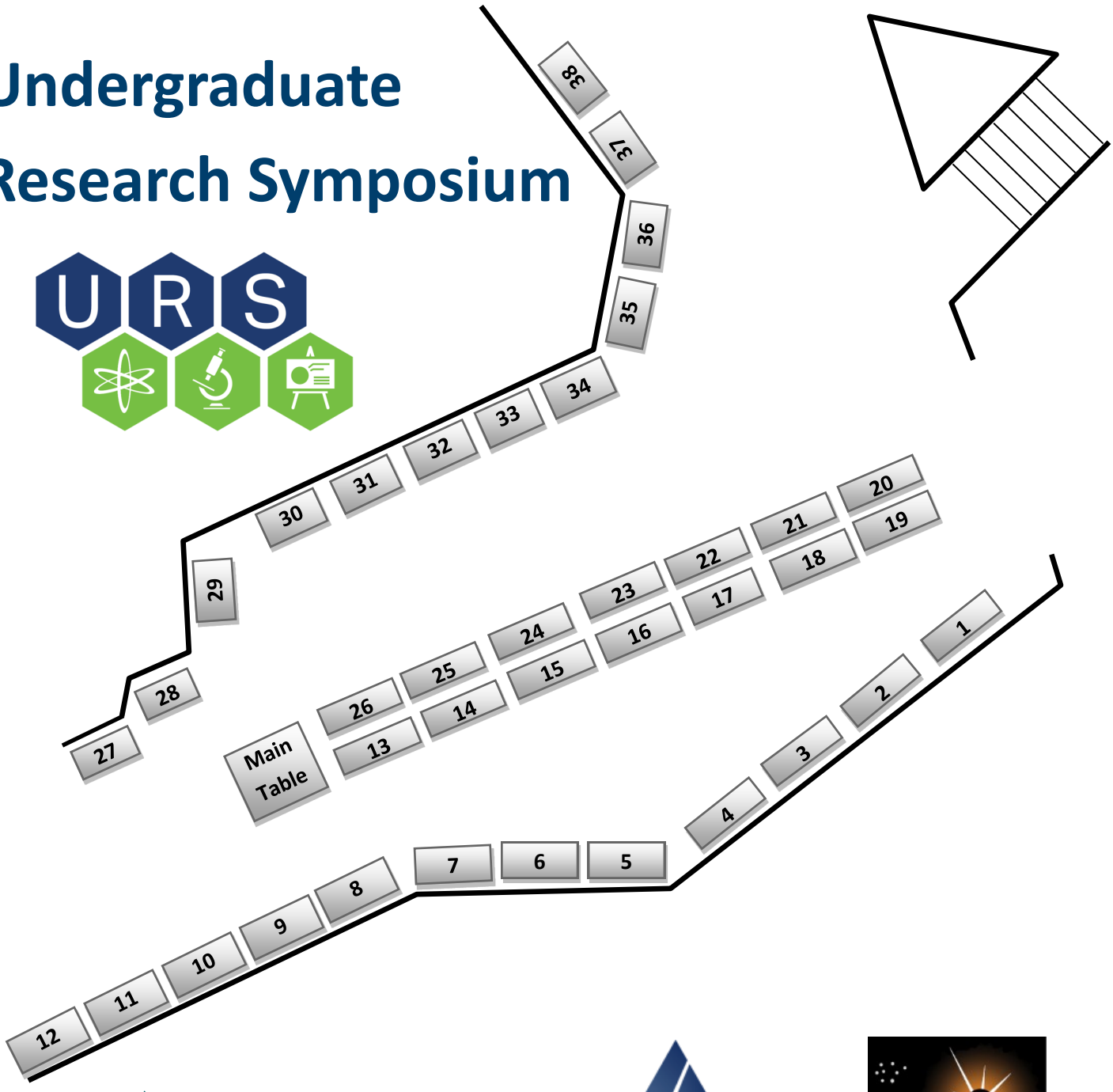

SURF

The Pavlis Honors College would like to welcome you to the 2017 Undergraduate Research Symposium!

The research presented here is sponsored in part by the Office of the Vice President of Research, the Portage Health Foundation, the DeVlieg Foundation, the Michigan Space Grant Consortium, the Pavlis Honors College, and the Summer Undergraduate Research Fellowship program.

SESSION A: 1-3 PM

	Presenter	Department	Title
1	Kaelan Anderson	Applied Physics	Studying the Properties of Free Tropospheric Aerosols in the Mid Atlantic
2	Dakota Anderson	Biomedical Engineering, Electrical Engineering	Improving Upper-Body Muscle Conditioning While Training at Low Intensities
3	Alicia Ball	Chemical Engineering	Effect of pH & Mineral Chemistry on Settling of Mineral Particles
4	Jared Bazile	Biochemistry & Molecular Biology - Chemistry	Generation and Expression of BAF180 Cancer-Associated Mutants
5	Brian Burtka	Chemistry	Engineering Metal Oxide Surfaces for Efficient Hydrocarbons Separation: a Quantum Chemical Study
6	Erica Coscarelli	Environmental Engineering	Impact of Dissolved Organic Matter & Its Transformation to Ultraviolet Photolysis Process in Engineered Water & Wastewater Treatment Systems
7	Aaron Dean	Mechanical Engineering	Effectiveness of Using SHRP2 Naturalistic Driving Study Data to Analyze Driver Behavior at Highway-Rail Grade Crossings
8	Kira Ferguson	Applied Ecology & Environmental Science	Integrated Social & Ecological Study on the Potential of Cognitive & Structural Fixes for Enhancing Local Urban Bee Populations
9	Mary Elizabeth Galbraith	Chemical Engineering	Unconventional Rare Earth Element Resources
10	Rebekka Guyon	Geological Engineering	Production of Biocementation from the Stimulation of Iron-Oxidizing Bacteria to Mitigate Dust Susceptibility
11	William Hughes	Mechanical Engineering	Investigation of Fuel Injection Systems-Fundamental Nozzle Cavitation Studies
12	Emily Hunt	Materials Science & Engineering	3D Printed Super-Bainitic Steel
13	Joe Iwanicki	Anthropology	The Archaeology of Trade: A Study of a Twentieth Century Logging Camp
14	Michelle Kelly	Environmental Engineering	Within-Reach Variation in Nitrification and Denitrification Rates in Lake Superior Tributaries
15	Ami Kling	Biomedical Engineering	Determination of the Effects of Hyperthermic Ablation on the Microstructure of Type I Collagen
16	Abigail Kuehne	CCM/Psychology	Trust & Cognitive Abilities: Human Factors' Impact on Cybersecurity Practices
17	Courtney Kurkie	Exercise Science	Sleep Efficiency & 24-hour Blood Pressure Patterns in Older Adults

18	Anthony Marcich	Mathematics, Applied & Computational	Preliminary Work for Autochrome Photograph Reconstruction: Scanning and Processing Design
19	Hannah Marti	Biomedical Engineering	Psychophysiological Effects of Acute Mindfulness Meditation (change to session 2 if other project stays in)
20	Allysa Meinburg	Biomedical Engineering	Sensorized Suture Anchor for Real Time Monitoring of Tensile Loads
21	Alex Miltenberger	Applied Geophysics	Multiple-Point Geostatistical Simulation of Fracture Networks Using Secondary Ground Penetrating Radar Information
22	Zachary Oldenburg	Chemical Engineering	A Preliminary Economic Feasibility Study for the Recycling of Lithium-Ion Batteries
23	Trevyn Payne	Chemical Engineering	Separation of Individual Components from Lithium-Ion Batteries
24	Emily Petersen	Materials Science & Engineering	Emergence of Home Manufacturing in the Developed World: Return on Investment for Open-Source 3-D Printers
25	Denada Planaj	Geological Engineering	Modeling Shallow and Deep Seated Landslides in Wayanad District, Kerala, India.
26	Sydney Smuck	Exercise Science	Smart Exercise Application with Wearable Motion Sensor: Validity & Usability
27	Samantha Stokes	Wildlife Ecology & Management	Assessing Mammalian Assemblages Along Senegal's Largest Artisanal Gold Mine
28	Violet Thole	Materials Science & Engineering	Structure Property Relationships in Next Generation Ballistic Fibers
29	Brittany Turner	Psychology	Assessing the Impact of Age-Related Declines in Implicit Memory Processes on Motor Learning.
30	Ben Updike	Chemical Engineering	Preliminary Quantum Chemical Investigations on the Designing of Effective Catalysts for the Haber Process
31	Joseph Vermeylen	Chemistry	Titan: A Novel Higher Tensile Strength Nacre-Like Material
32	E. Yasmine Walton-Durst	Mathematics	Rayleigh–Bénard Convection in Michigan Tech's Cloud Chamber – A Statistical Analysis of High Frequency Temperature Fluctuations
33	Travis Wigstrom	Chemical Engineering	A Better Approach to Tritylation of Alcohols
34	Jacob Schoenborn	Biological Sciences	Blueberry Protects Pancreatic Beta Cells

1. Studying the Properties of Free Tropospheric Aerosols in the Mid Atlantic

Student Presenter: Kaelan Anderson, Applied Physics
Faculty Advisor: Claudio Mazzoleni, Environmental Optics Laboratory

Introduction:

Long term research of atmospheric aerosols is necessary to accurately understand and predict a variety of atmospheric phenomena. A relevant example is black carbon, and its forcing effects on the climate. The Pico mountain atmospheric research observatory is a long running remote field site on mount Pico in the Portuguese Azores. Its focus is the observation of air pollutants, and aerosols from north America and Europe.

Materials and Methods:

The main objective of the project was the operation and maintenance of the research station. This is of importance, because the Pico mountain research station is located in the center of the north Atlantic Ocean at an elevation of 7,713 feet, which allows it to sample air that has been transported over long distances in the free troposphere. At this station we collect: nephelometer data at 3 wavelengths, black carbon concentration, aerosol absorption at 7 wavelengths, and particle number concentrations. The station is subjected to extreme environments and operates seasonally, meaning it must be closed for the winter and re-opened come spring. It is also necessary for a researcher to be on the island for frequent repair of the station. The secondary research was the ongoing collecting elevation profiles using portable instrumentation (nephelometer, aethalometer, particle counter, etc..).

Results and Discussion:

Claudio Mazzonleni, and I arrived on Pico on May 10th 2016, and by May 18th we were able to restore power, and major functionality to the station. The next month was spent restoring minor functionality, maintaining major functionality, and adding functionality. This included but not limited to bringing the meteorological station online, replacing the aethalometer, and adding a transformer for external cameras. Also during this month a few successful runs of the portable instrumentation were made, however due to continual poor weather conditions on the mountain this was only done a small number of times. The rest of the trip was spent preparing the station for running unattended the rest of the summer, and for the eventual winter conditions. I left the island on July 9th. The station ran for a few months powered, however the cable was damaged and has not been repaired by the locals as was discussed. However, we were able to continue the data set for part of the summer as hoped.

2. Improving Upper-Body Muscle Conditioning While Training at Low Intensities

Student Presenter: Dakota Anderson, Biomedical Engineering, Electrical Engineering (minor)
Faculty Advisor: Dr. Steven J Elmer, Kinesiology and Integrative Physiology

Introduction:

Resistance exercise via negative eccentrically-induced work (RENEW) serves as a high-force, low-cost, exercise for improving lower-extremity muscle conditioning (size, strength, power, mobility) in athletic and patient populations. We extended the RENEW model to the upper-extremities (RENEW-U) and evaluated the effectiveness of a 7-week intervention to improve upper-extremity muscle strength and power.

Materials and Methods:

Sixteen young healthy individuals performed either RENEW-U (n=8) or traditional concentric-based exercise (TRAD, n=8) training (3x/wk) while duration and intensity progressively increased in the same manner for both groups (5-20 min, ~60-70% of HR peak, RPE of ~13). Maximum upper-extremity power and isotonic elbow extensor strength were assessed before and one week after training. At the end of training total work for RENEW-U was ~2.5x that of TRAD (173±69 vs. 73±22 kJ, P<0.01). Muscle soreness associated with the exercise training was minimal and did not differ between RENEW-U and TRAD (0.42±0.41 vs. 0.27±0.37 cm, respectively, P=0.88).

Results and Discussion:

Compared to pre-training values, maximum elbow extensor strength increased (~11%, p=0.01) and maximum upper-extremity power tended to increase (~5%, p=0.08) for the RENEW-U group. There were no improvements in maximum elbow extensor strength or maximum upper-extremity power for the TRAD group. These preliminary results are promising in that repetitive multi-joint eccentric contractions with the upper-extremities might improve muscle strength and power even while training at only a "somewhat hard" effort, which parallels previously reported RENEW findings in lower-extremities.

3. Effect of pH and Mineral Chemistry on Settling of Mineral Particles

Student Presenter: Alicia Ball, Chemical Engineering
Faculty Advisor: Lei Pan, Chemical Engineering

Introduction:

Tailings are waste products from the mining, paper and chemical industries, and exit as low solid concentration slurries of fine particles. For example, the mining industry produces fluid mineral tailings ranging between 5 and 7 billion tonnes per year worldwide, with billions of tonnes already stored globally. Dewatering of these fine mineral tailings is challenging due to a low settling rate, particularly when particle size is below 5 μm. As a result, tailings are often directly discarded into impoundments for disposal. Dry stacking technology is an emerging method for producing dried cakes with a moisture content of typically less than 10% that can be transported by conveyors or trucks. It is a solid-liquid separation technology that combines flocculation and filtration processes. This project focuses primarily on sedimentation, in which we have fundamentally studied the settling of various mineral particles and how pH affects the rate.

Materials and Methods:

Sedimentation tests were conducted with different samples using a standard jar test experiment coupled with a GoPro vision system. Mineral samples including kaolinite, silica, alumina, iron oxide, and graphite, were tested. Polyethylene oxide was used as the flocculant. In each experiment, a slurry was prepared by mixing 5 g dry particles with 100 mL distilled water to obtain a 10% solid, and the solution pH was adjusted using hydrochloric acid or potassium hydroxide. The mixed slurries were transferred to a graduated cylinder and allowed to settle by gravity. We used a vision system to record the event of particle settling, and the videos were analyzed to obtain both the sedimentation rate and the floc sizes. Zeta potential measurements for various mineral particles were examined using a Malvern NanoZS, and the data was used to construct energy potentials between two particles in water.

Results and Discussion:

We have examined the effect of pH and surface chemistry of particles on the settling of particles in water. Our result showed that particles at a lower pH settle faster. The settling rate are different for particles of different chemistry. When using flocculants, particles settle much faster due to an increase in particle size. The larger the floc is, the faster particles settle. The present results will be interpreted using energy diagrams based on the DLVO theory. Future studies will be conducted to examine the effect of flocculants on settling.

DeVlieg Foundation

4. Generation and Expression of BAF180 Cancer-Associated Mutants

Student Presenter: Jared Bazile, Biochemistry and Molecular Biology - Chemistry
Faculty Advisor: Dr. Martin Thompson, Chemistry

Introduction:

Human polybromo-1 protein (BAF180) is a very large and complicated protein, which is mutated in more than 30 types of cancers. Two BAF180 mutants were selected for study, one of which occurred in a case of clear cell renal cell carcinoma (PD3492a) and the other in a breast cancer case (OC-314); both mutants result in deletion of most of the BAF180 protein. Comparison of the binding specificities of the cancer-associated mutant and full-length BAF180 will allow for a better understanding of the effects of mutants inside the cancer cell, which will eventually lead to better treatment options for cancer patients.

Materials and Methods:

PCR (polymerase chain reaction) is a common biochemistry technique that is used to generate many copies of a desired DNA sequence; it is being utilized to generate several BAF180 mutants that have been identified in cancer. The mutants will then be digested with restriction enzymes and ligated into the pET30a vector. After ligation, the mutant BAF180-pET30a construct will be transformed into E. coli DH5α cells for propagation. Rosetta(DE3) cells (also E. coli) will be used to express the mutant BAF180 proteins.

Results and Discussion:

Both of the mutants chosen, PD-3492a and OC-314, are around 900 bases. When performing gel electrophoresis for visualization of the PCR reaction product, bands around 2.0 kb were observed. This was thought to be a result of erroneous amplification (i.e. amplification of the wrong DNA sequence) New primers were designed to minimize the possibility of erroneous amplification. The implementation of these new primers resulted in bands approximately 1.5 kb. Manipulation of PCR conditions was not able to create 900 bp fragments, so it was hypothesized that the presence of secondary DNA structures was making the PCR products run slower than expected. The 1.5 kb products will be purified and ligated into pET30a. This BAF180-pET30a construct will be transformed into E. coli cells. Finally, the finished product will be sent in for sequencing for verification of formation of the mutated proteins.

5. Engineering Metal Oxide Surfaces for Efficient Hydrocarbons Separation: A Quantum Chemical Study

Student Presenter: Brian Burtka, Chemistry
Faculty Advisor: Loredana Valenzano, Chemistry

Introduction:

Current industrial processes for filtering crude oil revolve around cracking, the step where long-chain hydrocarbons are cracked into smaller, and more useful, hydrocarbons. These species contain alkanes, alkenes, and alkynes that are currently separated via cryogenic distillation. Given the dramatic difference in temperature between the two consecutive industrial process, the current procedure is extremely costly both energetically, and economically. More efficient methods have been recently sought. Among others, physisorption is considered the most promising with Metal Organic Frameworks (MOFs) potentially playing an important role in this quest. While MOFs have been proven to be very promising for such task, they decompose in the presence of water. Metal oxide surfaces resembling the adsorption sites present in MOFs are more stable, but they do not necessarily differentiate between the different guest molecular species. This project is aimed at designing and engineering metal oxide surfaces able to predict the separation potential that MOFs show with respect to light hydrocarbons.

Materials and Methods:

The planewave-based Quantum Espresso (QE) package was used to geometrically relax the bulk MgO 3D structure using the PBE-vdw density functional together with ultrasoft pseudopotentials. Metal oxide surfaces were then cut from the pre-optimized bulk material with Virtual NanoLab (VNL). The surfaces obtained consisted of three, five, seven, and nine layers. The slabs were geometrically relaxed to ensure converge with respect to the bulk limit. In order to avoid interaction between the adsorbing molecules, a supercell approach was employed. The complex formed by the five-layer supercell and the adsorbing molecule was then further relaxed by freezing the geometrical positions of the deepest four layers, and allowing for relaxation of the top two layers and the molecules only. This procedure allows for computational efficiency of the calculations while still preserving the required accuracy of the results.

Results and Discussion:

The first accomplishment came from relaxing the bulk structure. As standard procedure requires, the kinetic energy cutoff (KEC) for the wave functions and Monkhorst-Pack k-point grids were tested to ensure accuracy and computational efficiency. The best KEC was found to be 60 Rydbergs (Ry); the best grid for the bulk was found to be (8, 8, 8). These parameters were then used to calculate the total energy of the relaxed slabs. While the KEC cutoff was kept the same, the k-point grid was reduced to (1, 1, 1). The five-layer supercell slabs were found to successfully converge to the bulk limit. As hypothesized, our results for the molecular binding energies for C2-C4 confirm that the carbon chains with more degrees of unsaturation bind stronger to the surface, and that the larger molecules bind stronger than the small one. In addition, our results clearly indicate that the binding energy is very sensitive to the orientation of the hydrocarbon on the surface; this aspect will be further explored in the future.

6. Impact of Dissolved Organic Matter and its Transformation to Ultraviolet Photolysis Process in Engineered Water and Wastewater Treatment Systems

Student Presenter: Erica Coscarelli, Environmental Engineering
Faculty Advisor: Dr. Daisuke Minakata, Civil & Environmental Engineering

Introduction:

Presence of trace concentration of organic contaminants such as pharmaceutical and personal products, endocrine disruptor chemicals, so called emerging contaminants, raised public concern about water. UV photolysis is a well-established disinfection process attenuating these emerging contaminants in part as alternative to conventional chemical disinfections due to the little formation of disinfection byproducts. However, the presence of background dissolved organic matter (DOM), complex mixtures of organic matter, can decrease the removal efficiency of the target contaminants. We aim to characterize the transformation of standard humic substances during UV photolysis and understand the impact to the photolysis of a model organic contaminant.

Materials and Methods:

To test the degradation of Suwanee River Humic Acid (SRHA) and Fulvic Acid (SRFA), standard humic substances, a bench-top photoreactor with a 25W low-pressure UV lamp was used. Within the photoreactor the flow remained completely mixed to ensure uniform light exposure. The overall light intensity was measured using a ferrioxalate actinometry and obtained as Einstein/L•s. The local photon distribution was measured by a spectroradiometer. Solutions that contained approximately 10 mgC/L of either SRHA or SRFA will undergo photolysis and an aliquot of samples was taken at a certain time interval. Total dissolved carbon concentration was monitored with a TOC analyzer. The formation of low molecular weight organic acids will be measured with ion chromatography. Orbitrap UHR-MS will be used to characterize the complex mixture of OM which gives atomic ratios for H/C, O/C, and N/C for the compound found in solution. This data will be plotted as van Krevelin diagrams to analyze changes throughout photolysis.

Results and Discussion:

From the van Krevelin diagrams for both SRHA and SRFA as photolysis progresses, the H/C ration increases. This may be a result of increased saturation of carbon as the carbon-carbon double bonds are broken during photolysis. The O/C ratio increases in both samples as the length of photolysis is increased. This is most likely due to the organic compounds undergoing partial oxidation as they degrade. Knowing these preliminary results can allow for the understanding of how these compounds will react in the presence of H_2O_2, a commonly used oxidant. The next step in fulling understanding the impact that DOM has on treatment objectives is to determine how they alter removal efficiencies of target compounds with and without the addition of oxidants. These continued experiments will allow engineers to understand the potential byproducts of UV photolysis involving DOM as well as allow them to adjust dosage based on DOM concentrations to ensure that treatment objectives are continuously met.

DeVlieg Foundation

7. Effectiveness of Using SHRP2 Naturalistic Driving Study Data to Analyze Driver Behavior at Highway-Rail Grade Crossing

Student Presenter: Aaron Dean, Mechanical Engineering
Faculty Advisor: Dr. Pasi Lautala, Michigan Tech Rail Transportation Program

Introduction:

Highway-rail grade crossing collisions and fatalities have been in decline, but a recent ‘plateau’ has caused the Federal Railroad Administration (FRA) to concentrate on decreasing further casualties. The Michigan Tech Rail Transportation Program has been selected to perform a large-scale study that will utilize the SHRP2 Naturalistic Driving Study (NDS) data to analyze how various crossing warning devices affect driver behavior and whether there are clear differences between the effectiveness of the warning devices.

Materials and Methods:

It has been proposed that the machine vision head tracking data from the NDS will be used to evaluate driver looking behavior as they approach grade crossings. However, a conclusive method for validating the head tracking data has yet to be seen. It is still unknown whether or not the machine vision data has accurately recorded the driver head rotation characteristics. In an effort to validate the machine vision head tracking data collected during the NDS, it will be compared to a 'coded' narrative of driver looking behavior from the participant facing video.

Results and Discussion:

The main results of this study are the development of a coding scheme for the visual narrative, used to validate machine vision head tracking data, and an improved baseline for the head tracking data using a bivariate probability density function. Head tracking data from the NDS and its correlation with coded narratives are vital to analyze driver behavior as they traverse crossings. This project also presents preliminary results for the comparative analysis of the head tracking data from an initial test sample. Future work will extend the analysis to a larger data set, and ensure that use of the head tracking data is a viable tool for the ongoing behavior analysis work. Based on preliminary results from testing of the first data set, it is expected there will be significant positive correlation in future samples and the machine vision head tracking will prove consistent enough for use in the large scale behavioral study.

SURF

DeVlieg Foundation

8. Integrated Social and Ecological Study on the Potential of Cognitive and Structural Fixes for Enhancing Local Urban Bee Populations

Student Presenter: Kira Ferguson, Applied Ecology and Environmental Science
Faculty Advisor: Kathleen Halvorsen, School of Forest Resources and Environmental Science and Social Sciences Department

Introduction:

Ninety percent of angiosperm species require some sort of pollination by animals, most commonly by bees. Wild and domestic bees are important agriculturally, and are therefore economically important. In recent years there has been increasing evidence that bees, wild and otherwise, are in decline. Urban areas continue to spread, increasing the importance of studying bee populations in such areas. Urban bees are greatly affected by humans and their choices, specifically when it comes to landscaping. Human beliefs and values impact their conservation practices.

Materials and Methods:

I therefore coupled a study of pollinator populations, looking specifically at hymenoptera (bee) species with a sociological study to determine if cognitive or a structural fixes or a combination of them had great impacts on homeowners' bee-related behaviors.

Results and Discussion:

After participating in the study, homeowners were somewhat more likely to report behaviors encouraging pollinators but slightly less likely to view pollinators positively. This was a proof of concept study. Future studies should include a wider range of homeowners over a longer time span to allow the fixes a better chance at affecting the pollinator populations.

9. Unconventional Rare Earth Element Resources

Student Presenter: Mary Elizabeth Galbraith, Chemical Engineering
Faculty Advisor: Timothy Eisele, Chemical Engineering

Introduction:

A way to bypass the environmental stress and various procedures to separate raw earth from the REE is to work with materials that already contain the elements desired, yet currently are throw away as waste. Such materials include coal byproducts, clay minerals, red mud, and phosphorous materials. This report outlines practices of extraction REE from waste currently, the downfalls of each method, and ultimately will define the best economical and practical method of procuring REE from waste materials. Along with exploring these four byproducts, possible alternative routes of extraction will also be discussed.

Materials and Methods:

Thorough research was conducted using online databases such as ProQuest to gather information regarding 4 different waste materials for a literature review. From these sources, the best were chosen and then read through in order to procure the best information vital to the review.
Outside of the literature review, laboratory work was done. In the lab, phosphatic clay was acid leached in various concentrations and over various time frames to see if any of these variables change the effectiveness of REE extraction. ICP analysis was used to find the rare earth elements that had been extracted and their amounts.

Results and Discussion:

This report followed four methods of extracting rare earth elements from waste products. Coal ash shows promise of retrieving REE especially Ga and Ge under certain circumstances. Clay materials are a good source of REE when extracted using a Cs-based lixiviant, but the ores presented a challenge – the negative cerium anomaly. Red mud has uses other than the separation of REE including building materials and agricultural feedstock. Many problems were encountered with red mud processes because iron has a competitive extraction with REE causing the metal to REE concentrations to be extremely biased. Phosphogypsum is a byproduct of the fertilizing industry and utilizes the waste that would otherwise be sitting and causing potential harm to nearby water. Recrystallization poses problems due to increasing impurities in each subsequent layer. For all the methods, environmental waste streams were of concern along with impurities tagging along with the REE extraction. Each method uses harsh environments for extraction and varies in time and temperature. In terms of practicality and economics, each method utilizes leaching and uses common laboratory acids like HCl and H_2SO_4. From here, research will be conducted on phospogypsum to determine regeneration of results and the effect of changing multiple variables for better yields.

DeVlieg Foundation

10. Production of Biocementation from the Stimulation of Iron-Oxidizing Bacteria to Mitigate Dust Susceptibility

Student Presenter: Rebekka Guyon, Geological Engineering
Faculty Advisors: Drs. Eric Seagren, Stanley Vitton, and Thomas Oommen, Civil and Environmental Engineering

Introduction:

Mine tailings are byproducts of ore extraction in the mining industry, which are typically deposited as a slurry in massive impoundments. These tailings present several potential hazards, including dust emissions of fine-grained tailing particles (≈10 microns or less) under certain conditions. In addition, dust emissions pose many human health and environmental risks, including respiratory diseases and the contamination of water sources. Conventional dust mitigation methods have several limitations. The goal of this research is to evaluate an innovative bio-mediated mitigation approach based on stimulating iron-oxidizing bacteria (IOB) to form a bio-cemented surface, strengthening the tailings surface and reducing dust emissions.

Materials and Methods:

Gel-stabilized gradient tube experiments were performed to evaluate sources of IOB, and iron sources. Two types of iron oxide tailings – magnetite and hematite – were obtained and tested for their potential as an IOB source. The third potential IOB source was collected from a putative iron-oxidizing microbial mat found in a drainage ditch in Houghton, MI. The three potential inocula were tested with four different iron sources – iron sulfide (FeS), hematite tailings, magnetite tailings, and the field sample. The gel-stabilized gradient tubes used to test different combinations of inocula and iron sources contained two layers – the top layer consisted of a gelatinous-agarose mineral medium, while the bottom layer was the iron source. The inoculum of IOB was inserted near the interface between the layers. Then gradient tubes were sealed with a headspace. As oxygen diffused from the headspace into the agarose gel upper later, an oxygen gradient formed that decreased in concentration with depth. At the same time, iron diffuses upward from the iron source. If microaerophilic IOB are present in the inoculum, they will migrate through the agarose-gel mineral medium layer to favorable oxic conditions and iron concentrations, and grow; this is observable by the development of a particulate meniscus.

Results and Discussion:

Preliminary results obtained to date are promising. Five gradient tubes clearly produced a visible meniscus – all had hematite tailings as the iron source, with four having an inoculum of hematite tailings and one having the field IOB source as the inoculum. In addition, samples with the FeS plug and all inoculum sources also displayed signs of biological activity based on the oxidation of the FeS plug, and the cloudy yellow agarose top layer. These results indicate that neutrophilic IOB are present within the putative iron-oxidizing microbial mat inoculum, as well as the hematite and magnetite tailings. These findings have a number of implications for future work with IOB. Specifically, the promising conditions will be explored further in larger scale inoculated sample boxes undergoing typical compound surface conditions. If successful, IOB may create a durable surface crust that is resistant to wind erosion, providing an effective, inexpensive, and sustainable alternative for dust mitigation at mine tailing impoundments.

11. Investigation of Fuel Injection Systems- Fundamental Nozzle Cavitation Studies

Student Presenter: William Hughes, Mechanical Engineering
Faculty Advisor: Dr. Jeff Naber, Advanced Power Systems Labs, Alternative Energy Research

Introduction:

Cavitation of fuel within a DI fuel injector, despite much research, is not a well understood phenomena which can result in uncompensated changes in fuel injector characteristics. These changes have detrimental impacts on fuel economy, power and emissions. This investigation of cavitation will be conducted by using a modified fuel injector to accommodate a production injector sized transparent nozzle tip. By varying parameters known in typical engines, and recording flow via high speed micro-photograph, a correlation between given values and cavitation can be drawn. This correlation could predict, and thus compensate for cavitating flows found in DI engines.

Materials and Methods:

This modified fuel injector and production injector sized transparent nozzle tip will be mounted within an optically accessible constant volume combustion chamber; the resulting cavitating flow, and spray formation will be captured. By varying injection parameters and operating conditions experiments can be carried out to validate a variant of the cavitation number or Reynold's number as a predictor of fuel cavitation and thus changes to the discharge coefficient and spray formation for a given injector geometry. By running tests scaled by this value, cavitating flows that match those of typical diesel engine operating conditions, as well as hypothetical worst case conditions can be evaluated with a real scale transparent nozzle.

Results and Discussion:

The research, validation of hardware, and test matrix have all been completed to date. By the time of the research symposium all testing hardware will be in the lab, and testing will have been started, and possibly finished. Once complete these tests will provide insight into cavitating flow within fuel injectors which can be used by engineers in the computational fluid dynamics as well as engine calibration fields to produce better CFD codes and more robust engine calibrations to better meet emissions regulations, fuel economy and power targets through a reduction in variance as a product of fewer uncontrolled operating conditions.

12. 3D Printed Super-Bainitic Steel

Student Presenter: Emily Hunt, Materials Science and Engineering
Faculty Advisors: Dr. Joshua Pearce and Dr. Paul Sanders, Materials Science and Engineering

Introduction:

Reaching yield strength on the order of gigapascals is usually only something found in ceramics. However, the bainite phase in specially composed steel can be heat treated at low temperatures for longer times to reach yield strengths over 1GPa. By 3D printing this steel using Michigan Tech's GMAW method, steel parts can be made and machined easily, then heat treated to obtain these strengths. Making the steel this way will significantly reduce costs, especially when the temperature needed for the heat treatment is only 125C, low enough to cook a pizza!

Materials and Methods:

The steel will be swaged and drawn into 0.03" wire to be printed using the CNC 3D printer. After printing, the buttons will be cut off of the substrate and the surfaces ground down. Before the heat treating, the buttons will be encapsulated in quartz, flushed with argon gas to prevent oxidization. The heat treatment consists of 2 days at 1200C, 20 minutes at 1000C, and 2 months at 125C. Once the heat treatment is complete, multiple characterization methods will be performed: optical microscopy, hardness and compression testing, scanning electron microscopy. energy dispersive spectroscopy, and X-ray diffraction. While the samples are being heat treated, research into energy analyses of furnaces at low temperatures and industries with waste heat will also be conducted.

Results and Discussion:

During heat treatment, a phase transformation should occur resulting in retained austenite and at least 60% bainite, which is configured into nano-scale platelets. The shape of the microstructure, along with the crystal structure of this phase should result in yield strengths on the order of gigapascals. A cost analysis should show that this steel is worth the extra time to make, because the printing method used is far less expensive than CNC milling or powder printing and heating a furnace to 125C does not take up much energy.

13. The Archaeology of Trade: A Study of a Twentieth Century Logging Camp

Student Presenter: Joe Iwanicki, Anthropology
Faculty Advisor: LouAnn Wurst, Social Science - Archaeology

Introduction:

Trade and commodity flows are important in understanding how goods reach customers. This project uses archaeological data from a 1900's lumber camp in the Munising Michigan area called Coalwood. The data consists of artifacts that allow for investigation of trade and commodity flows. The archaeological record is combined with GIS to map and recreate the trade networks of the past, something rarely explored by archaeologists. This project also looks at the local, regional, national, and international ways of trade and how that affects what the people in Coalwood had as material culture, another aspect archaeologists don't often look at.

Materials and Methods:

The methods of this project can be categorized into three sections: archaeological, archival, and GIS. Archaeology is the main part of this project, over 40,000 artifacts were recovered from the archaeological excavation. These artifacts were washed, dried, cataloged, and entered into a database. The database was then used to sort locations of where the artifacts were from. These artifacts that had been separated out by location were put into their own file to be used in the GIS program. The GIS program couldn't be created just yet, archival research had to be done first. Using the MTU, NMU, and FU archives the major rail lines, shipping ports, mailing stations, and breweries were located. These give routes to how different goods would be placed in the GIS program. With the combined archaeological, and archive data the GIS program was started. The GIS program was created by using the oral history, archive work, and the material culture. Objects from the archaeology were placed on one of the trade networks that they would've followed. This allows the object to be traced from where they came from all the way to Coalwood.

Results and Discussion:

Archaeologists have rarely looked at the archaeology of trade and commodity flows. There has been work done by Adams, but he wants people to help flush out this type of archaeology more. This project lays down a groundwork of going about this type of archaeology. Specifically, understanding what methods should be used, expanding off of Adam's ideas. However, there is problems with this project when applying it to archaeology outside of industrial archaeology. This project revolved around extensive archival data to recreate the trade networks and to get the best trade network for each different material in the archaeological assemblage. If this data were not around, this project would've been extremely difficult and the results would be pure speculation. That is why the closer to current day the archaeology is for this type of work, the better the results will be. The data from the archive will allow for a better recreation of the trade networks. This project is important in creating a way for other archaeologists to look at a section of material culture that is mostly glossed over. This project gives archaeologists methodology as to how to figure this question out.

14. Within-Reach Variation in Nitrification and Denitrification Rates in Lake Superior Tributaries

Student Presenter: Michelle Kelly, Environmental Engineering
Faculty Advisor: Amy Marcarelli, PhD, Biological Sciences

Introduction:

Variation of biological nitrogen transformation rates among channel units within streams is assumed to be small, but has been seldom quantified. We asked whether nitrification and denitrification rates varied among channel pools within stream reaches, and how rates related to characteristics such as sediment organic matter and nutrient concentration.

Materials and Methods:

Sediment and water samples were analyzed from five pools within three first-order, low nitrogen streams in the Upper Peninsula of Michigan, using nitrapyrin-inhibition to quantify nitrification and acetylene block to quantify denitrification.

Results and Discussion:

Denitrification rates averaged three orders of magnitude lower than nitrification rates across all sites (5.10 x 10-4 vs 0.89 mg N m-2 hr-1). Rates measured in the smallest study stream showed greater variation among pools (CV = 6.3 and 2.0 for denitrification and nitrification, respectively) than rates measured across all pools in all streams (CV = 2.0 and 0.9), while variability among pools in the other two streams were similar to that measured across all streams. Our findings suggest that rates of nitrogen transformations may be highly variable among channel units and therefore may not be well estimated by a single study site per reach.

15. Determination of the Effects of Hyperthermic Ablation on the Microstructure of Type I Collagen

Student Presenter: Ami Kling, Biomedical Engineering
Faculty Advisor: Jingfeng Jiang, Biomedical Engineering Department

Introduction:

Thermal ablation is a minimally invasive cancer treatment technique which has the potential to allow clinicians to specifically target and eradicate tumors by causing intense localized heating and irreversibly damaging targeted tissue. Heating of Type I collagen – the most abundant fibrous protein within animal tissues – is thought to induce a change within its microstructure, leading to macroscopic structure changes and an elevation in measurable mechanical stiffness. The relationship between the thermal dose a tissue receives and resultant stiffness change allows for the development of imaging methods to more accurately delineate ablated tissue during the course of thermal ablation therapy.

Materials and Methods:

The sample material tested in this project was ex vivo pig liver tissue obtained from a local butcher. The tissue was cut into cubes approximately 1.3 cm on each side and heated to predetermined temperatures utilizing a temperature-controlled water-bath. Samples within the control group were placed in a 37°C isothermic bath to mimic physiological conditions. Experimental samples were subjected to a varying range of temperatures and time increments in order to simulate hyperthermic ablation. Creep and stress-relaxation tests were performed upon the samples post-ablation and tissue response (stress/strain) data from these tests were fit to a three-parameter Kelvin-Voigt Fractional Derivative (KVFD) model of tissue viscoelasticity. This change in tissue stiffness was then correlated to the thermal dose received during ablation simulation.

Results and Discussion:

"Analysis of experimental results verifies the mathematical relationship between thermal dose and a measurable increase in mechanical stiffness of the tissue. This in turn supports the nonlinear relationship between the thermal dose received during ablation therapy and the amount of collagen microstructure denaturation as a result of heating. Irreversible damage was found to occur at ablation temperatures equal to or above 60°C.

Many tumors are in locations that are difficult to delineate with traditional imaging techniques such as ultrasound and MRI; therefore, clinicians need a reliable method to determine amount of tumor elimination via ablation. The experimentally derived relationship between thermal dose and mechanical properties of ablated tissue may be used in order to develop new imaging techniques to reliably determine the amount of cancer cells/tissue destroyed by thermal ablation during the course of treatment."

16. Trust and Cognitive Abilities: Human Factors' Impact on Cybersecurity Practices

Student Presenter: Abigail Kuehne, CCM/Psychology
Faculty Advisor: Dr. Adam Feltz, Cognitive and Learning Sciences

Introduction:

Through internet activity, the world's communication not only in business relations, but also in casual conversation has shifted to email, online banking and social media. With this change in communication, people have become vulnerable in a new way to threats to their privacy and security resulting billions of dollars lost to internet crime and identity theft. My work attempts to help understand the human factors that increase vulnerability to these attacks. In particular, trust and cognitive abilities appear to be two major predictors of being susceptible to phishing attacks. By determining the connection that allows/prevents the end user to susceptibility of phishing, we can implement interventions to help people protect themselves.

Materials and Methods:

While a great deal of effort has been devoted to purely technical solutions to cybersecurity, one major and under-explored aspect of safe cyber practices are the dispositions, attitudes, and cognitive abilities of end users. Two major factors are trust and general decision making skill. Trust of a site allows for the production of a safe and productive future decision, and in turn, access to the link; it will also deter the user from generating a careless decision if the user believes that the information presented will not yield a negative consequence involved with the decision. Based on previous experience where information was skewed, trust will also determine what process should be acted upon. Testing for the trait of trust is integral to decision making and holds importance through determination of how a person reasons decisions that are not perceived as risky. There are multiple measures of trust as well as personality that have been assessed by our research that have generated a comprehensive collection of data. Analyzing this data will determine the propensity trust has in relation to phishing and internet crime.

Results and Discussion:

The data presents trust having a relation to phishing. Interpretation of the resulting data from the SPSS showed that the no phish 1 and 0, and phish 1 and 0 conditions had moderately strong correlations to the Rotter, Evans and Revelle, Couch, and BNT scales. For the no phish conditions, Rotter's r=.205 and r=.189 were respective to Evan's trust of r=.134 and r=.226, and Couch's r=.199 and r=.152. For the phish conditions, Rotter's r=.214, Evan's trust of r=.248, Couch's r=.254, and the BNT's r=.186 comparatively uphold a significant relation. This means that trust predicts making a decision to act on a phishing scheme, whether it be acceptance of the scheme or recognition of the scheme and avoidance of the situation. The Wilcoxin test specifically demonstrated a significant difference between phished and non-phished conditions. In the phished condition, the site looked extremely alike to the reliable and true site that your personal information would be processed. In the non-phished condition, the appearance of the phishing site or email was more transparent and was more easily recognized as a site that would steal your information. Further research to continue solving this issue may include how these phishing attacks can be prevented through the implementation of trust preventative measures.

17. Sleep Efficiency and 24-hour Blood Pressure Patterns in Older Adults

Student Presenter: Courtney Kurkie, Exercise Science
Faculty Advisor: Dr. Jason Carter, Kinesiology Department

Introduction:

Young adults with higher sleep efficiency (SE) have been shown to have greater reductions of systolic arterial pressure (SAP) and heart rate (HR) at night when compared to young adults with lower SE. SE becomes progressively worse with age, thus the purpose of the present study was to examine the association between SE and nocturnal dipping of SAP and HR dipping in older adults. Based on associations observed in young adults, we hypothesized that high SE (>85%) would be associated with greater reductions of nocturnal SAP and HR when compared to low SE group (<85%).

Materials and Methods:

Fourteen older adults (age range 55 – 75 years; 7 males, 7 women) were grouped into low (n=7) and high (n=7) sleep efficiency based upon 9 days of actigraphy. On a separate day of testing, 24-hour ambulatory blood pressure was recorded.

Results and Discussion:

Age (61±2 vs 61±2 years) and BMI (26±1 vs 28±1 kg/m2) were not different between the low and high SE groups (p>0.05). Total sleep time (TST) was significantly higher in the low SE group when compared to the high SE (7.7±0.2 vs 6.8±0.3 hours, p= 0.020). 24-hour SAP (125±6 vs 123±4 mmHg), DAP (75±3 vs 75±2 mmHg), and HR (70±3 vs 64±3 beats/min) were not different between low SE and high SE groups (p>0.05). Nocturnal dips tended to be higher in the low SE group than in the high SE group for SAP (15±2 vs 10±2%, p=0.073), DAP (19±3 vs 13±2%, p=0.096), and HR (22±2 vs 15±3%, p=0.073). In summary, and contrary to our initial hypothesis, high SE was not associated with greater reductions of nocturnal SAP and HR. Furthermore, the low SE groups spent more time in bed than the high SE group. This raises the question of the importance of TST versus SE of sleep in older adults.

PHFoundation

18. Preliminary Work for Autochrome Photograph Reconstruction: Scanning and Processing Design

Student Presenter: Anthony Marcich, Mathematics, Applied & Computational
Faculty Advisor: Cecile Piret, Mathematical Sciences

Introduction:

Autochrome Lumiere is the earliest commercially-successful color photography process. A unique feature of autochrome photographs are their composition of fine primary-colored points. Our goal is to use Radial Basis Functions methods (RBF) to construct smooth and accurate images from scans of these photographs. Our investigation of RBF requires processing scanned photos into nodes. Here we describe the initial scanning and processing work necessary to obtain these nodes.

Materials and Methods:

Consumer flatbed scanners lack the required resolution to clearly image autochrome grains (points). Our solution is a home-built scanner. This involves the construction of a CNC (computer numeric control) X-Y carriage and DSLR camera mount. This scanner captures numerous photos that can be combined in post-processing. Each photo requires processing removal of radial lens distortion and node identification. This is followed by a “stitching” algorithm that correlates image edges such that they can be combined together. It should be noted that these items are works in-progress- as such only our methodology will be described where applicable.

Results and Discussion:

Our calibration and processing will allow for high-resolution scanning using digital cameras. Our algorithms and methodology may be useful for others. Each procedure step offers a choice between processing conventional image matrices, or an analogue applied to scattered node features. This realization of a bimodal image processing methodology may be important for general applications.

19. Psychophysiological Effects of Acute Mindfulness Meditation

Student Presenter: Hannah Marti , Biomedical Engineering
Faculty Advisor: Dr. John Durocher, Biological Sciences

Introduction:

Anxiety is one of the most common mental health disorders in the United States. This disorder is strongly and independently associated with hypertension, arterial stiffness, and cardiovascular disease. Mindfulness meditation is often used to assist in the treatment of anxiety, however there is little known about the psychophysiological effects of a single meditation session. The purpose of this study is to clarify the effect of acute mindfulness on the cardiovascular system of anxious individuals. Clearly understanding the effects of mindfulness on the cardiovascular and cognitive systems, could help to improve the design of anti-anxiety therapies and interventions.

Materials and Methods:

In this study, we will collect baseline anxiety and cardiovascular data. Anxiety will be measured by the Beck Anxiety Inventory (BAI) survey. This is a 21-item self-report survey on a four-point scale, which examines the subject's anxiety and how much they are bothered by those symptoms. Only participants with BAI scores of 8 or higher (mild to severe anxiety) at the orientation session will be eligible for the testing and intervention. Cardiovascular variables to be measured are blood pressure, heart rate, heart rate variability, and arterial stiffness. Arterial stiffness will be assessed as augmentation index and pulse wave velocity obtained through applanation tonometry. We will also assess aortic pulsatile load (aortic pulse pressure * heart rate), which is an emerging risk factor for cardiovascular disease. The participant will then be guided through a 1-hour mindful meditation session. This session will include an introductory breathing session, guided body scan, and self-guided meditation. Immediately following the practice, the same cardiovascular testing will be repeated. Testing procedures will then be repeated again at 60 minutes, post intervention to measure potential time responses. Finally, the BAI survey will be administered again one week following the meditation practice.

Results and Discussion:

All data will be analyzed with commercial software (SPSS, IBM, Armonk, NY). A Repeated-Measures ANOVA procedure will be utilized to compare major dependent variables (ex: blood pressure, arterial stiffness, and anxiety) across the conditions (ex: baseline vs. post-meditation). Means will be considered to be significantly different when $P < 0.05$. We hypothesize that even a single, brief mindfulness meditation practice will have positive cardiovascular and psychological effects, by reducing aortic pulsatile load and anxiety according to the BAI. The overall purpose of this study is to clarify the effect of acute mindfulness on the cardiovascular system of anxious individuals. By having a better working understanding of the effects that mindfulness has on the cardiovascular and cognitive systems, we would be able to assist with designing therapies and interventions for those with anxiety disorders.

PHFoundation

20. Sensorized Suture Anchor for Real Time Monitoring of Tensile Loads

Student Presenter: Allysa Meinburg, Biomedical Engineering
Faculty Advisor: Dr. Keat Ong, Department of Biomedical Engineering

Introduction:

The ability to monitor force loading on a surgery site offers invaluable information to assist medical care personnel to optimize the healing time and outcomes of rotator cuff surgeries. Our goal is to create a passive force load sensing device to use within a bone screw and to be monitored over the course of healing. This will create a higher success rate in rotator cuff surgeries and can be further used in other surgeries involving a stressed healing environment. Our research focuses on the development and testing of a force sensing device within the bone screw itself.

Materials and Methods:

The force sensing unit is designed to be a passive design and actively monitored. The unit is made of layered magnetoelastic metal strips and secured on a flat hooked wire. The unit is hung by medical grade suture thread within two coils: an excitation circuit and a detection circuit. The unit was created to work in series with a function generator, amplifier and spectrum analyzer. The magnetic permeability of the magnetoelastic unit increases with the increased stress, and can be monitored through harmonic detection. The information is recorded and analyzed through Visual Basic software. Multiple sensors with different designs were constructed, and the performance of these sensors were characterized to determine the optimized design.

Results and Discussion:

The magnetoelastic detection strips were found to be an effective way to monitor force change. The magnetic permeability is agitated by a change in the force applied to the strips; an increase in force results in an increased magnetic permeability. The most effective sensors were the sleekest and most uniformly stacked magnetoelastic strips; the uniformity of the strip stacks were found to be a detection factor. The placement of the detection coil in relation to the excitation coil when reading the output of the sensor was also found to be factor in steady readings. Overall, the sensors were found to be a reliable way to record changes in force loads on the sensor. When completely developed, the described sensing system can measure loads applied to the bone screw and suture.

21. Multiple-Point Geostatistical Simulation of Fracture Networks using Secondary Ground Penetrating Radar Information

Student Presenter: Alex Miltenberger, Applied Geophysics
Faculty Advisor: Dr. Snehamoy Chatterjee, Geological and Mining Engineering and Sciences

Introduction:

Knowledge of the spatial arrangement of subsurface fracture networks can be valuable in many disciplines. Fracture networks help determine fluid pathways which are crucial in the study of groundwater flow and contaminant transport, and may provide information about geologic history, and much more. Ground penetrating radar (GPR) is one tool that can be used to gather information about subsurface fracture networks, but its interpretation can often be subjective or incomplete. This research proposes a stochastic geostatistical approach to interpreting fracture networks from GPR information with quantified spatial uncertainty.

Materials and Methods:

The multiple-point geostatistical simulation algorithm wavesim (Chatterjee et. al, 2012) is a stochastic spatial simulation procedure that operates by extracting patterns from an exhaustive data set, known as the training image, and matching those patterns to simulate an incomplete data. In this research wavesim was modified to incorporate two training images; a primary image with information about fracture location and a secondary image with GPR information. The patterns from these images were used to simulate a fracture location image from conditioning GPR information. Discrete fracture networks (DFNs) were created by discretizing the output from the program FracSim3D (Xu & Dowd, 2010). Eight DFNs were created from four statistical DFN parameter sets, with two realizations from each set. The GPR response to the DFNs was then simulated using the finite-difference time-domain algorithm developed by Irving and Knight (2006). Basic post-processing techniques were applied to the GPR response to improve the image quality using MatGPR (Tzanis, 2016). For each parameter set, the fracture and GPR information of one realization were used as training data, and the GPR response of the other realization was used as conditioning data to simulate, using wavesim, the fracture locations from the response.

Results and Discussion:

The results of the simulations found that the modified wavesim algorithm was able to identify fracture locations from the GPR response when the primary and secondary information had very high spatial correlation. In practice, it is very difficult to produce precisely correlated images of fracture networks from GPR information because of artifacts from the GPR acquisition procedure, primarily diffraction hyperbolas, and the post-processing techniques. Time-to-depth conversion is also difficult in practice because it requires prior knowledge of the subsurface electrical properties, yet is crucial in creating spatially correlated images. In addition, the resampling procedure applied to create images of matching dimension also skewed the steeply-dipping fractures to appear as scattered, discontinuous, flat features unrepresentative of true fractures. This research opens up the door to multiple-point pattern-based geophysical inversion. Applying rotation and translation functions, and other transformations, may reduce the need for highly correlated images.

22. A Preliminary Economic Feasibility Study for the Recycling of Lithium-Ion Batteries

Student Presenter: Zachary Oldenburg, Chemical Engineering
Faculty Advisor: Dr. Lei Pan, Chemical Engineering

Introduction:

Lithium-ion batteries (LIBs) use several high-value virgin materials within their battery chemistry, including active cathode materials (e.g., lithium cobalt oxide) and active anode materials (e.g., graphite). A recent study by Clean Energy Manufacturing Analysis Center suggests that the raw materials in a 30kWh LIB pack is valued at $4800-$6000. Our economic analysis is to evaluate contained values in the recycled product streams and processing costs for different recycling processes.

Materials and Methods:

In this work, we have surveyed 5 different LIBs used in electric vehicles (EVs) of different configurations and different active cathode materials. We compared the pros and cons of existing recycling technologies which are a pyrometallurgical process and hydrometallurgical process, as well as a new physical separation process we are currently developing in the laboratory. A preliminary study was conducted to compare a distribution of dollar values of each component in the LIBs and the contained values in the recycled product streams after different recycling process. In addition, an analysis is conducted to evaluate the operation costs of each process in recycling the spent LIBs, which include chemical costs, disposal costs and water treatment costs through a flowsheet design and a mass balance calculation. Net profits for each process will be calculated and a discussion on pros and cons of each separation process will be presented.

Results and Discussion:

We have shown that the physical separation of LIBs consumes a lower energy in processing and returns more value than other methods that are currently employed in the recycling industry. Physical separation maximizes the recovery of recyclable materials from the batteries. This allows recycled products to be a much more attractive feedstock than the mined ores. An employment of the physical separation system has a potential to be a financial success as well as a sustainable solution for battery recycling. Our preliminary study shows that a physical separation system can achieve 38% more value than a hydrometallurgical process, and 220% more value than a pyrometallurgical process. Improved recovery is attributed mostly to a recovery of active anode materials and full recovery of active cathode materials. While achieving more value, physical separation does not use any costly leaching and solvent extraction chemicals and has a nearly negligible operating cost.

23. Separation of Individual Components from Lithium-Ion Batteries

Student Presenter: Trevyn Payne, Chemical Engineering
Faculty Advisor: Lei Pan, Chemical Engineering

Introduction:

By the year of 2020, it is estimated about 300,000 t/y of batteries from electronic devices are available for recycling. This number will be doubled by the end of 2030, with additional 300,000 t/y of li-ion batteries (LIBs) from the automotive industry. Currently, the collection of batteries in U.S. is only a few percent of the total consumer LIBs. A majority of LIBs are disposed in landfills or shipped to other countries. The objective of this work is to develop an advanced physical and physiochemical separation method of recovering individual components from the spent LIBs while preserving components' function integrity. Preliminary studies on separation of components in the coarse and fine fraction from the shredded LIBs were studied.

Materials and Methods:

New Li-ion batteries were used as samples in this work. They were purchased from different venders, and came with different configurations and cathode materials. LIBs were first manually dismantled to remove steel casings, and it was followed by a shredding process in which the sizes of scraps were reduced to 5 x 5 mm. Both anode and cathode materials were separated from metal foils using a combination of kitchen blender and a mortar/pestle. Particle size and chemical composition of both cathode and anode materials were examined using Scanning Electron Microscopy (SEM). We have conducted laboratory-scale froth flotation experiments for both anode and cathode materials to demonstrate a feasibility of separation of different fine powders using a surface chemistry based separation process. The flotation results were compared with zeta potentials results obtained using a Nano ZS Zetasizer (Malvern).

Results and Discussion:

Zeta potential measurements showed that the electrokinetic properties of both cathode and anode powders behave very differently. The point of zero charge for LiCoNiOx and graphite powders are at pH = 3.5 and pH = 0.5, respectively. This result showed that LiCoNiOx and graphite can be separated at a pH between 0.5 and 3.5, where particles are oppositely charged. Zeta potentials of various cathode materials are currently under the investigation. Our laboratory-scale froth flotation tests showed that anode powders (i.e., graphite) can be separated from cathode powders using kerosene as the collector. We have shown that the recovery of graphite powders reaches above 90% after a 1-minute flotation time, while that for cathode materials is only 20%. Froth flotation tests with a mixed sample of anode and cathode materials are currently under the investigation.

Pavlis Honors College

24. Emergence of Home Manufacturing in the Developed World: Return on Investment for Open-Source 3-D Printers

Student Presenter: Emily Petersen, Materials Science & Engineering
Faculty Advisor: Dr. Joshua Pearce, Materials Science & Engineering

Introduction:

Through reduced 3-D printer cost, increased usability, and greater material selection, additive manufacturing has transitioned from business manufacturing to the average prosumer. This study serves as a representative model for the potential future of 3-D printing in the average American household by employing a printer operator who was relatively unfamiliar with 3-D printing and the 3-D design files of common items normally purchased by the average consumer.

Materials and Methods:

Twenty-six items were printed in thermoplastic and a cost analysis was performed through comparison to comparable, commercially available products at a low and high price range.

Results and Discussion:

When compared to the low-cost items, investment in a 3-D printer represented a return of investment of over 100%in five years. The simple payback time for the high-cost comparison was less than 6 months, and produced a 986% return. Thus, fully-assembled commercial open source 3-D printers can be highly profitable investments for American consumers. Finally, as a preliminary gauge of the effect that widespread prosumer use of 3-D printing might have on the economy, savings were calculated based on the items' download rates from open repositories. Results indicate that printing these selected items have already saved prosumers over $4 million by substituting for purchases.

25. Modeling Shallow and Deep Seated Landslides in Wayanad District, Kerala, India

Student Presenter: Denada Planaj, Geological Engineering
Faculty Advisors: Dr. Thomas Oommen & Sajin Kumar, Department of Geological and Mining Engineering and Sciences

Introduction:

Western Ghats, the passive continental margin of India, make up the west edge of Wayanad district. The plateau type geomorphology and tropical climate have resulted in the formation of clay rich soil. The steep slopes, high clay content, and the tropical climate have resulted in numerous slope failures. Deforestation, due to population increase, has negatively affected the slope stability as root cohesion has been reduced. Between 1961 and 2009 landslides have been responsible for 31 deaths and 103 families rehabilitated. The increased anthropogenic stress on the slopes are predicted to adversely affect the slope stability.

Materials and Methods:

To identify areas of slope stability, various spatio-temporal data was analyzed. A 30x30 meter digital elevation model (DEM) was derived from SRTM Imagery for analyzing the slope. Soil map and geotechnical characteristics were also studied in detail. Normalized difference vegetation index (NDVI) was extracted from Landsat 8 imagery and was necessary in correlating vegetation effects on landslide susceptible areas. All these layers were processed in ArcGIS, which facilitated the geospatial analysis. FORTRAN based probabilistic infinite slope analysis (PISAm), and Scoop3d were then used to calculate the factor of safety for slopes of the study area. These two programs were designed in such a fashion to study shallow, and deep seated landslides, respectively. The landslide susceptibility map thus derived was validated with the existing landslide inventory.

Results and Discussion:

The result derived from both PISAm and Scoop3d varies as the input parameters differ in both the methods. The correlation of the existing landslides between these models suggests that most of the landslides matches with PISAm model, designed for shallow landslides with a few matching with Scoop3d, which best fits for deep seated landslides. However, a couple of landslides had occurred in areas where slope was not steep. This validates that landslides were not influenced by a single parameter rather a combination of different parameters. On a broader sense, it can be concluded that the landslides which fits to these models corroborates with the classification of Zêzere.

Pavlis Honors College

26. Smart Exercise Application with Wearable Motion Sensor: Validity and Usability

Student Presenter: Sydney Smuck, Exercise Science
Faculty Advisor: Tejin Yoon, Kinesiology and Integrative Physiology

Introduction:

To improve the commitment levels of a home-based exercise program, a smart exercise application with a wearable motion sensor was developed.

Materials and Methods:

Study 1 explored the accuracy of the proposed sensor (MetaWear C, mbientlab, Portola, San Francisco, CA). Four subjects (20.5 ± 1.2 years) participated in this study. A fixed platform (size: 90 × 90 mm) was attached on subjects' abdomen where our sensor, a commercial accelerometer (Trigno wireless, Delsys Inc., Boston, MA), and reflector markers of motion analysis system (OptiTrack Prime 13; Natural Point, Inc., Corvallis, OR) were attached together. While participants were performing a lunge, the motion was recorded using 3 systems simultaneously. Body angle and 3 direction accelerations of our sensor were compared to motion analysis system and the commercial accelerometer respectively. Pearson's correlation and root-mean-square error (RMSE) were calculated to assess the accuracy of our sensor. Bland-Altman plots were also plotted to test discrepancy between two systems. Study 2 surveyed the usability of the smart exercise application using a questionnaire. Twenty-three subjects (23.3 ± 6.4 years) answered 8 questions related to exercise initiation and adherence after using the smart exercise application

Results and Discussion:

High correlations with low RMSE were observed between the sensor output and the reference output for the direction angle ($r = 0.99 \pm 0.01$, $p < 0.001$, RMSE= 5.12 ± 1.86˚) and for the x, y, and z-axes acceleration ($r = 0.91 \pm 0.03$, $p < 0.001$, RMSE = 0.13 ± 0.04 m/s2; $r = 0.91 \pm 0.04$, $p < 0.001$, RMSE = 0.18 ± 0.02 m/s2; $r = 0.92 \pm 0.02$, $p < 0.001$, RMSE = 0.23 ± 0.05 m/s2, respectively). Bland-Altman plot also showed a low discrepancy between two systems. In study 2, most of the participants (approximately 90%) strongly agreed or agreed to the questions related to interest, motivation, and convenience to exercise with our application. The sensor mimics similar qualities to that of commercial devices. In addition, a high rate of positive response suggested the success of the application in future use.

PHFoundation

27. Assessing Mammalian Assemblages along Senegal's Largest Artisanal Gold Mine

Student Presenter: Samantha Stokes, Wildlife Ecology and Management
Faculty Advisor: Kelly Boyer Ontl

Introduction:

Anthropogenically driven defaunation is a global epidemic. In Senegal, major threats to wildlife include habitat degradation, conversion, and resource competition. Increased artisanal small-scale gold mining, which attracts people from all over West Africa, exacerbates these threats. Since 2012 when Kharahena became the largest artisanal gold mining site in Senegal, its population has boomed from 150 to an estimated 30,000 inhabitants. Our research strives to construct a mammalian assemblage near Kharahena for the summer of 2016, building on previous research and assessing possible changes between 2011(pre-mining) and 2016 (post-mining) wildlife populations.

Materials and Methods:

Reconyx PC800 HyperfireTM cameras were deployed at two water sources located 2.5 km and 7 km from the mining area. The cameras were attached in plain view to trees facing the water sources at a height of 1m with Python LocksTM, and set to operate continuously for approximately six weeks. The cameras were set at the highest level of sensitivity for motion and temperature differential detection and took three photographs per trigger. Available images were sorted by camera location and wildlife species were identified and the quantified. Using basic count statistics and measurements of trapping success, we compared the results with the 2011 camera trap data. In addition to using camera traps, we conducted recce walks along dried riverbeds and trails to look for signs of mammals and evidence of human activity. Recce walks ranging from 1-18 km were conducted on nine days and were analyzed for presence/absence and encounter rates. Mammal encounter rates for each recce were weighted by survey effort.

Results and Discussion:

The effects of the 30,000 people living and working around Senegal’s largest artisanal gold mine can be seen across the landscape in huge shifts in land use and correlating ecosystem degradation. Clean water has become scarce due to pollution from unchecked population growth and use of water sources to crush ore. Bushmeat hunting has also increased; during our nine days in the field we saw seven different instances or hunting/fishing camps, shotgun shells or hunted animals. During a comparable survey in 2011 only three signs of hunting were observed. The relatively low number of mammal encounters, only 15 total over nine days, and low number of wildlife signs in general illustrate the negative effect secondary industries (palm wine production and timber extraction) have on wildlife populations whose home ranges they affect most heavily. Whole palm forests have been damaged for the production of palm wine. The process of palm wine collection removes the top of the tree to access the sap, killing the tree. Comparative analysis of a subset of camera trap images from 2016 to 2011 showed substantially larger numbers of humans, domestic animals, and timber harvesting which supports the growth of the mines and residential areas.

28. Structure Property Relationships in Next Generation Ballistic Fibers

Student Presenter: Violet Thole, Materials Science and Engineering
Faculty Advisor: Dr. Erik Herbert, Materials Science and Engineering

Introduction:

Improving the scientific community's understanding of the complex coupling between the structure and mechanical properties of polymer fibers will directly enable the successful development of next generation ballistic armor. Specifically, new knowledge is needed to better understand how common structural characteristics such as the mer unit, molecular weight, crosslink density, and crystallinity serve to limit the fiber's ability to dissipate mechanical energy. While nanoindentation is one of the primary characterization techniques used to measure energy dissipation, numerous experimental challenges associated with specimen preparation and modeling of the measurement system's dynamic behavior must be overcome in order to obtain accurate test results.

Materials and Methods:

To make suitable specimens for nanoindentation, cryogenic microtomy was used to create smooth and damage free test surfaces. Polyethylene and Kevlar fibers (20 μm diameter) were threaded through rubber molds that were backfilled with epoxy. Once cured, the epoxy supported fibers were placed into a Leica Ultra Cut Microtome and cooled to cryogenic temperatures, approximately -100 °C. Cutting the fibers in cross-section, the test surfaces were prepared in two stages, trimming and final facing. Numerous variables such as but not limited to temperature, knife angle, cutting speed, slice thickness, and epoxy hardness collectively control the quality of the microtomed surface. Ideal cutting conditions were only identified through extensive trial and error. The quality of prepared surfaces was assessed using optical, scanning, and transmission electron microscopy. Nanoindentation was used to measure the fiber's energy dissipation as a function of length scale, frequency, and temperature. Instrument characterization experiments were performed to determine the frequency range over which the instrument's motion could be accurately and precisely modeled by a single degree of freedom, simple harmonic oscillator. Over the frequency range of 40 to 200 Hz, experiments were performed in the fibers using a Berkovich indenter tip at indentation depths of approximately 100 nm.

Results and Discussion:

The quality of the bonded interface between the fiber and epoxy, scratches caused by damaged regions of the knife, "chatter" in the surface produced by poor cutting conditions, evidence of crystallinity, and microstructural damage at the free surface were all evaluated using optical, scanning, and transmission electron microscopy. The microscopy results clearly indicate the fibers are amorphous and that the free surface is not free from microstructural damage induced by the microtome. At indentation depths less than 60 nm, the measured damping shows a strong depth dependence that may be the result of or amplified by the microtome induced damage. Over the frequency range of 40 to 200 Hz, dynamic characterization of the nanoindentation system shows the actuator's motion can be accurately modeled as a single degree of freedom, simple harmonic oscillator to within ±3% or better. Over that same frequency range, the data also show the phase lock amplifier is configured such that the measured phase angle can be accurately predicted by the oscillator model to within ±2% or better. Collectively, these results can be used to construct well-defined lower limits on the contact dimensions that can be used to accurately measure the damping of polymer fibers using nanoindentation.

29. Assessing the Impact of Age-Related Declines in Implicit Memory Processes on Motor Learning

Student Presenter: Brittany Turner, Psychology
Faculty Advisor: Dr. Kevin Trewartha, Cognitive and Learning Sciences (Meese Center)

Introduction:

Motor learning is supported by separate fast and slow learning processes that allow for rapid, and more gradual improvements in performance, respectively. Recent evidence has shown that the slow process is impaired in older adults, leading to increased forgetting, and poorer performance relative to younger adults. It has been suggested that the slow processes rely on implicit memory processes, but there has been no direct support for this assertion. The current project investigated whether scores on an implicit memory test are correlated with the slow process and whether age-related declines in implicit memory are related to deficits in motor learning.

Materials and Methods:

For the current project, a group of younger adult undergraduate students (18-30 years old) from Michigan Technological University, and a group of healthy older adults (60-85 years old) from the Houghton, MI community were recruited to participate in a motor learning experiment investigating the impact of age-related declines in implicit memory on the slow process for motor learning. Participants performed a motor learning task in which they reached to visual targets while grasping a handle attached to a robot that generates unusual movement-dependent forces at the handle (KINARM, BKIN Technologies). Performance in the motor task was used to provide an estimate of the fast and slow learning processes. In addition to the motor tasks, participants performed a battery of cognitive tasks using PEBL (The Psychology Experiment Building Language), including a procedural learning task, known as the pursuit rotor task, which is known to rely on implicit memory mechanisms. Participants also completed two explicit memory tasks, including the paired-associates task (measuring associative working memory) and the corsi-blocks test (measuring spatial working memory). These explicit memory measures were used to ensure that age-related deficits in the slow process for motor learning are uniquely related to implicit, and not explicit memory.

Results and Discussion:

The main goal of the current project is to determine if age-related changes in implicit memory can account for previously observed declines in the slow process for motor learning in aging. The slow process can be estimated from the magnitude of the after-effects that participants experience after learning to counteract the forces imposed by the robot when reaching to visual targets. Correlations between procedural learning scores on the pursuit rotor task and the magnitude of the after-effects on the motor task were calculated to test two hypotheses: 1) that implicit, procedural learning resources underlie the slow process for motor learning in younger adults, and 2) that age-related deficits in implicit memory account for age-related declines in the slow process for motor learning. Our findings provide valuable information about the nature of age-related changes in motor behavior that can inform the design of interventions aimed at improving functional independence in later adulthood.

30. Preliminary Quantum Chemical Investigations on the Designing of Effective Catalysts for the Haber Process

Student Presenter: Ben Updike, Chemical Engineering
Faculty Advisor: Loredana Valenzano, Chemistry

Introduction:

The Haber process is the industrial process used to form ammonia from nitrogen (N¬2) and hydrogen (H2). More than 450 million tons of ammonia (NH3) are produced using this method every year. It is the single largest chemical production process and consumes 5% of the world's natural gas annually. The process uses metallic catalysts to increase the yield of ammonia and to speed up the reaction. These catalysts have been mostly unchanged since the process which was first developed in 1909. Improvements in catalyst design could speed up the process and lower activation energy, saving energy and money.

Materials and Methods:

Theoretical and computational chemistry techniques were employed to design the catalyst. Density Functional Theory (DFT) was used as the method for testing the structures. The planewave-based Quantum Espresso (QE) package was used to geometrically relax the bulk Vanadium 3D structure using the PBE density functional together with ultra-soft pseudopotentials. Subsequently, Vanadium (1,1,2) slabs were designed using Virtual Nanolab (VNL) and exported into Quantum Espresso format. The total minimum energy of the structures was obtained by geometrical relaxation. All Quantum Espresso calculations were carried out using MTU's Superior computing system. Important parameters such as K-point sampling, wave function energy cutoff, and number of layers present in the surface (from three up to seven) were determined using convergence tests on the simplest pristine surface models. The surfaces were then uniformly doped with nitrogen atoms, and H2 molecules with the former covalently coordinating five Vanadium surface atoms, and the latter sitting on top of the metal atoms. Different geometrical arrangements were imposed to the H2 molecules to determine the most stable solution.

Results and Discussion:

Optimum values for K-point sampling were determined (12, 12, 12) while the energy cutoff for the wave function was established at 60 Ry (Rydberg). The number of layers chosen for the surface was five. The Taffel dissociative mechanism for ammonia formation was chosen as the ideal reaction pathway for this study, and the stability of the different surface structures were addressed in a stepwise fashion. In other words, different static snapshots of the reaction path were investigated to address the stability of the intermediate states in ammonia formation (NH, NH2).

31. Titan: A Novel Higher Tensile Strength Nacre-like Material

Student Presenter: Joseph Vermeylen, Chemistry
Faculty Advisor: Loredana Valenzano, Chemistry

Introduction:

Nature offers a template to create biomimetic materials embodied with extraordinary properties. Among other necessities, species such as mollusks have developed hard shells characterized by composite structures formed of nacre. These provide a fascinating template to artificially engineer new, hard materials able to efficiently disperse energy from induced strain. This is different from ceramics, for example, which are very hard, but brittle materials. In this project, nacre constitutes the template to build a novel biomimetic, high tensile strength material made of graphene and Kevlar.

Materials and Methods:

The mechanical property known as tensile strength provides quantitative information about the amount of stress that a material can handle before fracture. In this work, the tensile strength of two different materials were used to test the most reliable computational model to predict the mechanical properties of the new graphene-Kevlar nacre-like material, Titan. Calculations were performed at electronic structure level by applying periodic boundary conditions (PBC) first to graphene and Kevlar alone, then to the original Titan material. The quantum chemical code, Gaussian09, was employed. Graphene (2D) and Kevlar (3D) periodic structures were anisotropically stretched to impose deformations ranging from 1% to 10%. Titan was manually built as a 3D structure according to symmetry considerations, and allowed to stretch from 1% to 10% along one of the three Cartesian directions. The tensile strengths of graphene and Kevlar were used to test the validity of the adopted theoretical approaches, and used as a solid ground to predict the behavior of the new hybrid material.

Results and Discussion:

The tests conducted on both graphene and Kevlar yielded a tensile modulus of 1.1 TPa, and 122 GPa, respectively. Both the results are in good agreement with experimental evidence with the latter value showing an overestimation of about 10% due to the difference between the complexities of the fiber-like, real structure of Kevlar with respect to the defect-deficient (perfect) model used in this project. To the best of the authors' knowledge, the result obtained for Kevlar, is original, and it appears to be the first attempt to provide a description of the mechanical properties of this material at quantum chemical level. Nevertheless, the major outcome of this investigation refers to the prediction of the tensile strength of the Titan structure, which yielded a tensile modulus of 23.1 GPa. This result is astonishing as it indicates that our new hybrid material dramatically overcomes the tensile strength of natural nacre by three orders of magnitude.

32. Rayleigh–Bénard Convection in Michigan Tech's Cloud Chamber – A Statistical Analysis of High Frequency Temperature Fluctuations

Student Presenter: E. Yasmine Walton-Durst, Mathematics
Faculty Advisor: Will Cantrell, Ph.D., Department of Physics, Atmospheric Science Program

Introduction:

Atmospheric physics is a field that allows for the development and use of comprehensive mathematical models. This research project is an ongoing contribution to a much larger study of atmospheric sciences, extending outside the walls of Michigan Technological University, using the cloud chamber experimental data. Taking advantage of the wealth of data produced by Michigan Tech's novel cloud chamber, this project has aimed at using time series analysis and other statistical methods to identify trends in temperature fluctuations from a second to several minutes. We hypothesize that data from the temperature sensors can provide a signature of the characteristic fluid movement within the chamber.

Materials and Methods:

The chamber creates artificial clouds lasting up to 26 hours and are induced using the same conditions that cause cloud formation in natural environments. Turbulent mixing clouds are the result of a high temperature floor and low temperature ceiling, which can be modeled by Rayleigh–Bénard convection. The warmer, lower density, fluid at the floor rises as colder, higher density, fluid from the ceiling falls and mixing occurs. The initial temperature gradient will eventually change and go towards zero as the fluids reach temperature and pressure equilibrium. Keeping boundaries in the chamber at a constant temperature allows for a constant temperature gradient, which allows for long term observation of cloud formation. The mixing causes turbulence and slight temperature changes that we aim to quantify.

Results and Discussion:

The focus of this presentation is explaining the computations and resulting analysis from Rayleigh–Bénard convection experiments using only the 8 temperature sensors sampling once per second. This is a simple method of reading between the numbers, but it is also just a starting point. Our data supports that increased temperature gradient results in a larger temperature variance, which is predicted by Rayleigh–Bénard convection models. The data output from Michigan Tech's cloud chamber is promising and can contribute to furthering mathematical models of cloud physics, turbulence, and fluid dynamics.

DeVlieg Foundation

33. A Better Approach to Tritylation of Alcohols

Student Presenter: Travis Wigstrom, Chemical Engineering
Faculty Advisor: Shiyue Fang, Chemistry

Introduction:

Trityl functions are a widely used functional group in organic chemistry. Trityl chloride is the most common way of introducing them. Trityl chloride unfortunately has the drawbacks of being expensive, moisture sensitive, harmful, and difficult to evaporate.

Materials and Methods:

The reaction is a two-step process with the first involving the formation of a carbocation and the second involving a reaction between the carbocation and the alcohol. The introduction of Trifluoro acetic anhydride to the initial trityl alcohol encourages the first step carbocation formation.

Results and Discussion:

The use of trityl alcohol as an alternative to trityl chloride mitigates manyof trityl chlorides drawbacks. The expensive nature of trityl group introduction is removed as expensive silver salts aren't needed for the carbocation formation. Trityl alcohol is also much more stable making handling it an easier process. The ease of evaporation also makes trityl alcohol much easier to use.

34. Blueberry Protects Pancreatic Beta Cells

Student Presenter: Jacob Schoenborn, Biological Sciences
Faculty Advisor: Dr. Xiaoqing Tang, Biological Sciences

Introduction:

The statement “the most powerful drugs for your body are the foods and beverages you eat and drink everyday” underlines the importance and influence nutrition has on our health. Evidence has demonstrated that imbalanced diet is a major reason for obesity and consequently type-2 diabetes. This makes it important to determine which diet is best for protecting the pancreas against the onset of diabetes. One such food is the blueberry. Blueberry contains antioxidants which have been shown to protect against oxidant-induced cell damage. In addition, blueberry is full of bioactive substances that help improve insulin sensitivity. Blueberry appears to affect pancreatic β-cells which regulate the amount of glucose in the blood and aid in the storage and secretion of insulin to reduce the glucose level. However, whether blueberry protects β-cell function and growth has not been fully evaluated.

Materials and Methods:

To investigate blueberry effect on beta cell function, a modified high-fat diet supplemented with 4% freeze-dried whole blueberry powder (HFD+B) and was fed to the C57BL/6 male mice. This was then compared to mice fed with a standard high-fat diet (HFD).

Results and Discussion:

The addition of blueberry had no significant change in the body weight and glucose level, but, after 8 weeks feeding, the plasma insulin level was decreased significantly in mice fed with HFD+B. In addition, mice fed with the HFD+B diet had an increased glucose tolerance and were more sensitive to insulin. The blueberry-supplemented diet also prevents the HFD-induced β-cell expansion and preserved the Islet of Langerhans structure within the pancreas of the mouse. When all of this is taken together, our results indicated that the blueberry diet could protect β-cells, restore impaired glucose homeostasis brought about by a HFD, and it could slow the development of obesity. These experiments will provide new insights into the effects of blueberry on β-cell function and our understanding of the importance of a balanced diet in treating and preventing obesity and diabetes.

SESSION B: 3-5 PM

	Presenter	Department	Title
1	Erica Anderson	Geological Engineering	Modeling the Potential Travel Paths of Post-Wildfire Debris Flows
2	Yani Beeker	Materials Science & Engineering	Open-Source Parametric 3-D Printed Slot Die System for Thin Film Semiconductor Processing
3	Quelyn Bekkering	Geology	Textural Analysis of Magmatic Fabrics Within the Princeton Caldera Ring Dike
4	Abbie Botz	Exercise Science	Total Sleep Deprivation and Sympathetic Neural Control in Older Adults
5	Katie Bristol	Applied Geophysics	Rock Magnetic Investigation of Carbonaceous Chondrules from the Allende Meteorite
6	Jeffrey Brookins	Materials Science & Engineering	Prototyping & Characterization of Zinc-Based Bioabsorbable Vascular Ligating Clips
7	Andrew Bruning	Mechanical Engineering	Generating Monodisperse Oxidized Methacrylated Alginate Microbeads with Specific Encapsulation Factors
8	Derek Burrell	Electrical Engineering	Performance Analysis of Stationary Hadamard Matrix Diffusers in Free-Space Optical Communication Links
9	Thomas Bye	Exercise Science	The Effects of Respiratory Muscle Fatigue on Upper-Body Exercise Performance
10	Stephanie Dietrich	Exercise Science	Subjective & Objective Assessments of Sleep Differences in Male & Female Collegiate Athletes
11	Elisha Earley	Biomedical Engineering	Evaluating Novel Biodegradable Stent Materials
12	Simon Eddy	Materials Science & Engineering	Tungsten Disulfide as a Counter Electrode in Dye-Sensitized Solar Cells
13	Alexis Ferrier	Chemistry	Synthesis of a Fructopyranose Mimic as a Carbohydrate Probe for Fructose Transporters
14	Brian Flanagan	Computer Engineering	The Effects of Uncertain Labels on Damage Assessment in Remotely Sensed Images
15	Meghan Friske	Biomedical & Electrical Engineering	Characterization of Electrospun Nanofiber Scaffold for Wound Healing Applications
16	Samuel Gaines	Civil Engineering	Structural Health Monitoring Using UAV's & Kinect Sensors
17	Drew Hanover	Mechanical Engineering	Building-to-Grid Predictive Power Flow Control for Demand Response and Demand Flexibility Programs
18	Jackie Harris	Chemical Engineering	Investigation into the Free Radical Scavenging Activity of Novel Nitroxide Derivatives
19	Madison Heeringa	Mathematics: Actuarial Science	Finding Structure in Data

20	Carly Joseph	Biomedical Engineering	Development of a Novel Injectable Nitric Oxide Releasing Fibrin Microgel Composite Hydrogel for Tendon Repair
21	Ryan Kibler	Environmental Engineering	Understanding Lake Superior Warming Through Observational Data & Model Results
22	Emily Lilla	Chemistry	Sulfenamide Form of Omeprazole in Interaction with the Primary Amino Acid Sites of H+/K+ ATPase as Investigated at Electronic Structure Level
23	Jeremy Luebke	Environmental Engineering	Changes in Tropospheric Ozone Formation With a Reduction in PM Over China
24	Hannah Maat	Exercise Science	What Do You Think Before You Fall?
25	Mary Kate Mitchell	Chemical Engineering	Predicting the Rejection Efficiencies of Toxicologically Relevant Organics in Reverse Osmosis of Wastewater Reclamation Processes
26	Kelci Mohrman	Physics	The Geminga Pulsar Wind Nebula and the Positron Excess
27	Madelyn Morley	Exercise Science	An Experimental Investigation of the Role of Spatial Working Memory in Age-Related Declines in Motor Learning
28	Charles Newlin	Materials Science and Engineering	The Effects of Nano-Sized Particles in Ultrahigh Carbon Steels
29	Thomas Page	Mechanical Engineering	Linear Traverse Design Project for Research Applications in the Cloud Chamber
30	Emily Praznik	Environmental Engineering	Macroinvertebrates in Hammel Creek
31	Hao Qin	Materials Science & Engineering	Synergistic Effect of Graphene-Oxide-Doping & Microwave-Curing on Mechanical Strength of Cement
32	David Ross	Biomedical Engineering	Covalently Bonded Collagen Coating on PDMS Improved Human Mesenchymal Stem Cell Sheet
33	Philip Staublin	Materials Science & Engineering	Modeling Biocorrosion of Zinc Alloys in Endovascular Environment
34	Valeria Suarez	Geological Engineering	Risk Assessment & Slope Stability Modelling of a Transportation Corridor in Hindu Kush Range
35	Trevor Taubitz	Computer Networking & Systems Administration	Assessment of the Personal Security State of Highly-Trained & Non-Highly-Trained Users
36	Brendan Treanore	Materials Science and Engineering	Substrate Active Cooling for Weld Based 3D Printing
37	David Trine	Biochemistry & Molecular Biology	The Role of the Genetic Toolkit in the Evolution of Complex Color Patterns of Drosophila Guttifera
38	Randall Wilharm	Chemistry	Synthesis and Characterization of Novel Photoactive Lanthanide Complexes

1. Modeling the Potential Travel Paths of Post-Wildfire Debris Flows

Student Presenter: Erica Anderson
Faculty Advisor(s): Dr. Thomas Oommen, Geological & Mining Engineering & Sciences

Introduction:

An increase in post-wildfire debris flow events has warranted the need for an improvement of current modeling techniques in order to better understand these hazards and their impact on critical infrastructure. To date, researchers have developed probabilistic models to predict potential locations and associated volumes of erodible material generated from the wildfire affected areas.

Materials and Methods:

This research works to supplement the previous modeling efforts by identifying the potential travel path of debris flows, utilizing the hydrology toolbox within ArcMap 10.4. The study evaluates 11 locations affected by wildfire with varying terrain conditions; three preliminary study sites and eight validation study sites. The basic assumption of this study is that the debris flow has a similar travel path to surface runoff, and thus by creating a flow accumulation layer from the 10m DEM, possible debris flow travel paths can be predicted. Preliminary results of this analysis looked at three study sites which had documented debris flow occurrences. Working within Google Earth historical imagery of pre and post wildfire dates at these study sites allowed debris flow scars to be identified and outlined. Analyses of the alignment between the modeled flow accumulation layer and these mapped debris flow scars were then performed. To validate the preliminary results, a total of 28 debris flow scars were analyzed.

Results and Discussion:

The end results show that the hydrology model works best with a more variable terrain, and at a Threshold Value of 50. A Threshold Value of 25 did model debris flow travel paths well, but at the risk of having an overestimation of results. The model was least accurate in mapping debris flow paths that were on the edge of the fire boundary, and at locations that had extremely flat terrains. However, lowering the threshold value to 10- 25 did allow for some accuracy to be found in modeling debris flow travel paths in flat terrains. Due to the simplicity of this model, it is recommended that this modeling technique be used in congruence with other information and analyses on the study site in question before any action is taken.

DeVlieg Foundation

2. Open-source Parametric 3-D Printed Slot Die System for Thin Film Semiconductor Processing

Student Presenter: Yani Beeker, Materials Science and Engineering
Faculty Advisor: Joshua Pearce, Materials Science and Engineering

Introduction:

Slot die coating is growing in popularity because it is a low operational cost processing technique for depositing thin and uniform films rapidly while minimizing material waste, which is straight-forward to scale-up for roll to roll processing. The complex inner geometry of conventional slot dies require expensive machining that limits accessibility and experimentation. In order to overcome these issues this study follows an open hardware approach with an open source 3-D printer to both fabricate the slot die and then to functionalize a 3-D slot die printing system.

Materials and Methods:

The slot die was modeled using the open source software, OpenSCAD, a script-based, parametric CAD (computer aided design) program possessing powerful 3-D modeling capabilities. The slot die was printed by an Athena build delta RepRap 3-D printer initially in PLA for geometric prototyping, which was later changed to (polyethylene glycol-co-1,3 cyclohexanedimethanol terephthalate) (PETG, from eSUN 3D) due to solution resistance testing. Due to the geometry, any other orientation would create overhangs, which are detrimental to the printing precision. This orientation also allowed for a sufficient area to be utilized as a base so adhesion to the print bed was adequate. After prototyping the slot die the final print settings were determined. The complete settings are in the supporting information. The G-code was exported from Cura and imported into the firmware, Franklin. The slot die was made to be compatible with a Prusa Mendel i1 RepRap 3-D printer. With the slot die mounted, a 1 mL syringe is then loaded into the slot die without the needle tip attached. The syringe pump (through Franklin) pulls the syringe end extending it and allows air to enter the syringe itself.

Results and Discussion:

The thickness, roughness, and percentage transmission for four samples has been measured. Using AFM values, the thinnest sample (A) had a root mean squared (RMS) roughness of 1.66 nm less than the thickest sample (D) for the 1x1 μm area. For the larger 10x10 μm area, this difference in roughness increases to 3.059 nm. It is also important to note that sample A is almost three times thinner than sample D (17 nm compared to 49 nm). Thus, by simply changing the extrusion rate the surface roughness and thickness may be modified or tuned for a specific application. Additionally, sample A displayed a transmission of about 99.1%, while the sample D showed a slightly lower transmission of about 94.5%. The ability to 3-D print slot dies provides many benefits in the research setting. Costs are significantly reduced when using this method. Commercially available slot dies of comparable sizes typically cost over $3,950. The slot die used in this experiment had a mass of 9 grams and at $25.95/kg for filament was produced at a cost less than a 25 cents in materials. This is a 17,173% decrease in cost.

3. Textural Analysis of Magmatic Fabrics within the Princeton Caldera Ring Dike

Student Presenter: Quelyn Bekkering, Geology
Faculty Advisor: Dr. Chad Deering, Geological & Mining Engineering & Sciences

Introduction:

An understudied constituent of large magmatic systems are ring dikes, which are formed during caldera collapse as large volumes of magma are evacuated. Because much of the magma has already erupted once caldera collapse has occurred, material from the deeper portion of the reservoir is squeezed up along the margins (ring dike) and can later be exposed for study. The Badger Creek eruption is directly related to unerupted magma that is exposed along a ring dike within the larger Princeton Batholith and is the focus of this study.

Materials and Methods:

"The following details how the combined use of Zircon U-Pb dating, scanning electron microscopy (SEM), electron backscatter diffraction (EBSD) and energy dispersive spectroscopy (EDS) will be used to construct a magmatic history: Dating zircons using radiometric dating of uranium (U) and lead (Pb) will enable us to construct a geochronology of the magmatic system, and determine the position of the ring dike in relation to other units. The integration of EBSD analysis into quantitative textural studies that couple output from EDS will allow us to identify a variety of physical processes occurring within magma reservoirs. The simultaneously collected EDS data is processed to identify phases (mineral assemblages) and document compositional variations within grains. Electron backscatter diffraction is a rapid method of measuring the crystallographic orientation. The EBSD data may be post-processed to a map and plot shape-preferred orientation (SPO) and lattice-preferred orientation (LPO) fabrics, as well as provide grain size and phase identification data. The EBSD data can be used to differentiate between fabrics formed by different processes by identifying foliations and lineations, such as: magmatic flow, compaction, gravitational settling, deposition from flowing slurries or density currents."

Results and Discussion:

Results from Zircon U-Pb dating has given us dates in concordance with a published study conducted by Mills and Coleman on this system in 2013. Our dates from plutonic lithics within the ring dike overlap in time with sample dates calculated by Mills and Coleman. Given that the quartz monzonite (a unit resulting from the magma found in our lithics) lies 10 km to the south of our sampling points for the ring dike, we know that this unit is quite extensive. From this, we can conclude that we have sampled from an earlier part of the magmatic system that was active prior to both the Badger Creek Tuff and the ring dike. Additionally, trace elements in the ring dike lithics have two distinct chemistries of zircons, showing us that we have samples from two distinct batches of magma. Because we now know that there is no assimilation of Precambrian crust, we can narrow our future studies to within the context of Mount Princeton. Our calculated dates, coupled with future integration of SEM, EBSD, EDS, and petrographic analysis of thin sections, will enable us to determine the magmatic system's history, as well as the scope of these processes.

Pavlis Honors College

4. Total Sleep Deprivation and Sympathetic Neural Control in Older Adults

Student Presenter: Abbie Botz, Exercise Science
Faculty Advisor: Jason Carter, Kinesiology

Introduction:

Epidemiological studies have suggested a link between sleep deprivation and hypertension. Our laboratory has recently shown that young women have a more negative sympathetic neural response to sleep deprivation than men. Given that the risk of hypertension increases significantly in women after menopause, we hypothesized that total sleep deprivation (TSD) would alter neural and cardiovascular responses in older adults, and that these alterations would be more dramatic in postmenopausal women.

Materials and Methods:

Fourteen participants between the ages of 55 and 75 years (8 women and 6 men) took part in this study. Subjects were tested twice within one month, once after 24-hour TSD in the laboratory and once after several consecutive nights of normal sleep. Wrist actigraphy was worn 5 days prior to each testing to confirm normal sleep patterns. We recorded muscle sympathetic nerve activity (MSNA) via microneurography, blood pressure via sphygmomanometer, and heart rate via electrocardiogram during 5 min of supine, awake rest.

Results and Discussion:

"TSD altered MSNA differently in older men and women (time × condition, $p = 0.035$). Specifically, TSD lowered baseline MSNA in older men (38±4 to 34±4 burst/min), but increased baseline MSNA in postmenopausal women (30±3 to 34±4 burst/min). Baseline blood pressure and heart rate responses to TSD were not significantly different between men and women ($p>0.05$). In summary, 24-hour TSD significantly increased sympathetic neural responses in postmenopausal women when compared to age-matched men, but the sympathoexcitation was not associated with an augmented pressor response."

PHFoundation

5. Rock Magnetic Investigation of Carbonaceous Chondrules from the Allende Meteorite

Student Presenter: Katie Bristol, Applied Geophysics
Faculty Advisor: Dr. Aleksey Smirnov, Geological and Mining Engineering and Sciences

Introduction:

According to some models, magnetic fields could have played an important role in the early solar system controlling the transfer of mass and angular momentum that resulted in the formation of Earth and its planetary neighbors. However, the strength and distribution of these magnetic fields remains poorly understood. The chondrules of carbonaceous chondritic meteorites represent the oldest material formed in the solar system. They start at high temperatures as dispersed molten droplets, which subsequently solidify and aggregate into chondritic bodies. Therefore, the chondrules may contain a record of early solar system conditions including evidence for ancient solar magnetic fields.

Materials and Methods:

The Allende meteorite, which fell over Mexico in 1969, is the largest and oldest (~4.567 billion year-old) carbonaceous chondrite ever found. Because of the recency, the Allende fragments have not experienced any terrestrial weathering. Initial magnetic investigations of the meteorite indicate that the original natural remanent magnetization (NRM) is preserved. This NRM provides quantitative evidence for the presence of a magnetic field in the early solar nebula but does not directly provide information on the field strength (paleointensity). I have investigated the magnetic properties of Allende meteorite chondrules to investigate their feasibility as paleointensity recorders. Approximately, 50 chondrules were separated from the parent body. The chondrules were repeatedly washed and ultrasonically cleaned to remove any remaining groundmass before beginning further analyses. Magnetic hysteresis parameters were measured from the chondrules using an Alternating Gradient Field Magnetometer (AGFM). The AGFM was also used to test the samples for magnetic anisotropy by comparing magnetic hysteresis parameters measured at multiple orientations with respect to the applied magnetic field. Finally, first order reversal curves (FORCs) were measured to determine the size distribution of magnetic minerals and magneto-static interactions between magnetically soft and hard mineral phases.

Results and Discussion:

Temperature dependencies of low-field magnetic susceptibility were measured by cycling from room temperature to 700C (in argon) using an AGICO MFK1-FA magnetic susceptibility meter. The curves were also measured during heating from -192C to room temperature before and after high-temperature thermomagnetic runs. Magnetic hysteresis investigations of the chondrules revealed the presence of nearly single-domain to pseudo-single domain ferromagnetic inclusions, lack of magnetic anisotropy, and other ideal characteristics for paleointensity experiments. However, the measured thermomagnetic curves were irreversible indicating that the chondrules experience severe thermal alteration upon heating. Thus, the conventional Thellier method is not suitable for paleointensity experiments on Allende chondrules. The results of my investigation suggest that, due to the vulnerability of the samples to thermal alteration, an alternative paleointensity method is needed to accommodate for the intricate mineralogy of the extraterrestrial samples. To eliminate the possibility of thermal alteration, my future work will include an alternative paleointensity determination method that does not require heat.

6. Prototyping and Characterization of Zinc-Based Bioabsorbable Vascular Ligating Clips

Student Presenter: Jeffrey Brookins, Materials Science and Engineering
Faculty Advisor: Jaroslaw Drelich, Materials Science and Engineering

Introduction:

During surgical operations, blood vessels are often severed to gain access to deeper portions of the body. For the prevention of bleeding, various methods of hemostasis are used; however, only ligating clips can be quickly applied while also withstand arterial pressures. Given recent advances, the medical device industry is increasingly looking toward new, biodegradable metals; rather than inert materials. In 2012, researchers at Michigan Technological University demonstrated that zinc is not only biocompatible, but also has an excellent rate of in vivo biodegradation; allowing for clips to be applied and then absorbed within months.

Materials and Methods:

The investigation of the zinc alloys followed a qualitative and quantitative process. This allowed potential candidates to be eliminated early in the process, without wasting labor-intensive resources. First, the alloys were initially evaluated using a simple bend test and microscopy techniques. By roughly forming the shape of the vascular ligating clip, with a small bending radius of only a few millimeters, stress cracking could be induced. With the aid of stereo- and electron microscopy, the tensile region of the bending radius was investigated for cracking. In order to measure the bursting pressure of the applied clips, a peristaltic pump was set to deliver 3 mL/min of water to tubing upon which a clip was applied. Using an arterial pressure transducer, the maximum pressure before failure was recorded. Finally, using dynamic materials analysis allowed for the flexural modulus (stiffness) to be measured at both room and body temperature, 23°C and 37°C respectively. This was determined using a calibrated three-point bending test.

Results and Discussion:

Initially, a promising zinc alloy was discarded due to large amounts of stress cracking within the tensile region of the clip's bending radius; leading to catastrophic fracture. Due to the composition of the alloy, and its low elongation, it is believed that the intermetallic microstructure is the main cause of this issue. While pure zinc (4N) did not exhibit any cracking, due to its higher elongation, the stiffness and burst pressure yielded further data for analysis. Currently, commercial clips are manufactured from titanium or stainless steels; providing high flexural, as well as tensile, strength. With the combination of burst pressure and flexural modulus, further work can be done to optimize the geometry of the clip's cross-section via finite element analysis or extrapolation methods.

7. Generating Monodisperse Oxidized Methacrylated Alginate Microbeads with Specific Encapsulation Factors

Student Presenter: Andrew Bruning, Mechanical Engineering
Faculty Advisor: Dr. Chang Kyoung Choi, Mechanical Engineering

Introduction:

Osteoarthritis affects millions of Americans resulting in billions of dollars spent on treatment. Functional articular cartilage must have depth dependent heterogeneity in cell morphology, pericellular matrix (PCM), chemical nutrients, extracellular matrix composition (ECM). Current tissue engineering is using a layer-by-layer method (3D printing), but it cannot control the chemical and mechanical stimulants simultaneously and heterogeneously. Encapsulating cartilage cells will promote desired ECM and PCM growth and morphology, which is critical to growing viable cells and tissues. This research provides a protocol for the generation of microgels. The manufacturing of microgels is the first step towards developing better cartilage tissues.

Materials and Methods:

The experimental setup consists of two liquid phases: an OMA phase solution and a mineral oil phase solution. The microfluidic devices used all had a X-junction layout and a constant channel width of 100 m. The channel heights used were 15, 20 and 40 m; the channel serpentine lengths were 2, 3, 4, 6 and 9 cm. The two phases were injected into the microchannel by flexible polyethylene tubing and two syringe pumps; the OMA phase tubing was wrapped in aluminum foil. The images of the droplets are obtained using a Nikon Eclipse Ti-U microscope in conjunction with a high-speed camera, and analyzed using imaging software. The droplets were cured using a UV light with variable UV intensity. The microchannel was held in a fixture that allowed the UV light to be easily “flipped” down into position. The fixture and oxygen scavenging packets were enclosed in a clear ZipLock bag that had holes for tubing, UV cord and nitrogen tube.

Results and Discussion:

Data is still being collected and the protocol is not complete. The process of generating microdroplets and then microgels has been very complicated. Some preliminary results show that the UV exposure time is more critical than the UV intensity, the threshold has yet to be determined. The first experiments aimed at determining the maximum flow ratio for steady monodisperse droplets for each channel length have now shifted focus to curability. We are interested in knowing if droplets can cure in a certain channel length at the maximum UV intensity and finding the lowest UV intensity the droplets can be cured at for that channel length. Finding the lowest UV intensity is important so microgels can be collected for a longer time. It has already been seen that the 2 cm microchip is too short and microdroplets do not have enough time to cure. This knowledge is valuable because it saves the chip manufacturer, Ph. D. student Shuo Wang, time and materials. Once the protocol is fully developed and robust the first step towards better manufacturing viable articular cartilage tissues will be complete.

8. Performance Analysis of Stationary Hadamard Matrix Diffusers in Free-Space Optical Communication Links

Student Presenter: Derek Burrell, Electrical Engineering
Faculty Advisor: Christopher Middlebrook, Electrical and Computer Engineering

Introduction:

Wireless communication systems that employ free-space optical links in place of radio/microwave technologies carry substantial benefits in terms of data throughput, network security and design efficiency. Along with these advantages comes the challenge of counteracting signal degradation caused by atmospheric turbulence in free-space environments. A fully coherent laser source experiences random phase delays along its traversing path in turbulent conditions forming a speckle pattern and lowering the received signal-to-noise ratio upon detection.

Materials and Methods:

The goal of the research being performed is to experimentally demonstrate and quantify improvement of signal-to-noise ratio for turbulence scenarios using a custom Hadamard diffractive matrix design to statically induce partial coherence in a transmitted beam. Atmospheric phase screens are generated using an open-source software package and subsequently loaded into a spatial light modulator using nematic liquid crystals to modulate the phase.

Results and Discussion:

Preliminary research has shown that receiver-side speckle contrast may be significantly reduced and signal-to-noise ratio increased accordingly through the use of a partially coherent light source. While dynamic diffusers and adaptive optics solutions have been proven effective, our solution proposes to reduce the expense and complexity of a system that relies on accessibility and robustness for successful implementation.

9. The Effects of Respiratory Muscle Fatigue on Upper-Body Exercise Performance

Student Presenter: Thomas Bye, Exercise Science
Faculty Advisor: Dr. Steven Elmer, Department of Kinesiology and Integrative Physiology

Introduction:

Respiratory muscles are used every minute of every day to generate force for breathing. During exercise, respiratory muscles are also used to stabilize the spine and torso. Therefore, controlling these muscles is important because of their dual roles in breathing and movement. However, it is currently unknown if respiratory muscle fatigue compromises upper-body exercise performance. The purpose of this study was to evaluate the effects of respiratory muscle fatigue on upper-body exercise performance. By carrying out the purpose we will have a better understanding of the respiratory system, elite sport performance, and exercise prescription for people with COPD and asthma.

Materials and Methods:

Four upper-body trained endurance athletes volunteered for this study. After a preliminary visit to establish their upper-body peak oxygen consumption (VO2peak) and peak power (Wpeak) participants performed two upper-body exercise trials. For the first exercise trial (control) participants performed "arm cranking" at ~85% of Wpeak until task failure/voluntary exhaustion (~10min). For the second exercise trial (pre-fatigued), participants performed the same task, but while having a pre-existing level of fatigue in their respiratory muscles greater than or equal to ~20% of their maximal inspiratory mouth pressure (MIP). This fatigue was induced by breathing through a hand-held resistive breathing device, which simulates lifting weights for the diaphragm muscle. Respiratory muscle fatigue associated with exercise was estimated by the pre- to post-exercise reduction in MIP. During the exercise trials, I recorded total work output in kJ, power, oxygen consumption, heart rate, ventilation, perceived effort, and shortness of breath.

Results and Discussion:

At this time, two participants have completed the study (VO2peak of 51±6 mL/kg/min, Wpeak of 205±25 W). For the control trial, MIP decreased by 13±4% (158±15 vs. 141±15 cmH2O) indicating that high-intensity upper-body exercise did severely stress the respiratory muscles. Time to failure from control trial to pre-fatigued trial decreased by 18±2% (13.7±2.3 vs. 11.2±1.6 min). Currently, these preliminary data support my hypothesis that upper-body exercise does induce respiratory muscle fatigue and supports lower-body findings from research. In addition, time to failure did decrease for these participants which allows me to speculate that during high intensity upper and lower-body exercise the metaboreflex may play a role in why performance decreases when respiratory muscles are fatigued. These findings have implications for researchers who use upper-body exercise to evaluate participants, clinicians who prescribe exercise for patients with COPD and asthma, and athletes who participate in full/upper-body sports. Because of a small sample the project is being continued until I reach ten subjects to test the current trend.

PHFoundation

10. Subjective and Objective Assessments of Sleep Differences in Male and Female Collegiate Athletes

Student Presenter: Stephanie Dietrich, Exercise Science
Faculty Advisor: Jason Carter, Department of Kinesiology and Integrative Physiology

Introduction:

A number of studies report that sex (i.e., male vs. female) can influence subjective and objective assessments of sleep. Specifically, women tend to report lower subjective sleep quality compared to men, yet objective assessment via actigraphy have shown a paradoxically higher sleep duration and sleep efficiency in women compared to men. The vast majority of work in this area has been limited to middle-age and older adults. Despite the importance of sleep in athletic performance, no studies to date have focused on young, healthy athletes.

Materials and Methods:

Based on data from the general population, we hypothesized that female athletes would demonstrate improved objective, and worse subjective, assessments of sleep when compared to men. A total of 36 collegiate varsity athletes (23 males, 20 ± 1 years; 13 females, 20 ± 1 years) were studied. Subjective assessments included sleep duration (sleep diary), Pittsburgh Sleep Quality Index (PSQI), and Epworth Sleepiness Scale (ESS). Objective assessments of sleep included three consecutive days of actigraphy to assess sleep onset latency (SOL), total sleep time (TST), sleep efficiency (SE), and wake after sleep onset (WASO), as well as one night of at-home ApneaLinkTM to determine the apnea-hypopnea index (AHI). Comparisons were made using independent t-tests.

Results and Discussion:

PSQI (6±1 vs. 6±1 units, p=0.907) and ESS (8±1 vs. 9±1 units, p=0.144) were not different between male and female athletes. In contrast to these subjective measures of sleep, several objective assessments of sleep were different between sexes. Both male and female athletes demonstrated lower TST than standard recommendations for young, healthy athletes, with a trend toward lower TST in female athletes (6.9±0.2 vs. 6.3±0.3 hours, p=0.058). In contrast, male athletes had significantly higher WASO (40±4 vs. 25±3 min, p=0.013), higher SOL (37±6 vs. 19±4 min, p=0.037), and lower SE (82±1 vs. 87±1%, p=0.004) compared to female athletes. Male athletes had a significantly higher AHI (1.1±0.2 vs. 0.4±0.1, p=0.028), but neither group had any subjects with clinically-defined sleep apnea. Finally, male athletes demonstrated a significantly greater mismatch between self-reported sleep duration and objective sleep duration (p=0.009). In summary, objective assessments of sleep were different in male and female athletes, yet both groups were below recommended levels of sleep for young, healthy athletes. These findings suggest that different sleep hygiene strategies and interventions may be necessary in male and female collegiate athletes to improve sleep duration and/or quality.

Pavlis Honors College

11. Evaluating Novel Biodegradable Stent Materials

Student Presenter: Elisha Earley, Biomedical Engineering
Faculty Advisor: Dr. Jeremy Goldman, Biomedical Engineering

Introduction:

Bare metal and drug eluting stents are often deployed to restore blood flow through diseased arteries. Although beneficial in the short term, the permanent presence of these traditional stents can be harmful for the artery. Biodegradable vascular implants made from zinc have been shown to harmlessly degrade at a rate to disappear within 1 – 2 years. However, high purity zinc lacks the mechanical strength needed for a stent. In an effort to overcome this limitation, we have added alloying elements to the zinc base to improve its mechanical properties without compromising its immunocompatibility.

Materials and Methods:

“We use a wire implantation model that simulates the presence of a stent in the vascular space. The wires are placed in the abdominal aorta of a rat by puncturing the arterial wall with the wire, advancing the wire through the lumen, and puncturing the wire out of the lumen at the far end. Upon explantation at different time points, wires and arteries are snap-frozen in liquid nitrogen and cryosectioned for histological analysis. Histological processing consists of an H&E stain to enable identification of neointima formations and measure their thicknesses, with statistical comparisons made between groups. This staining also allows for a determination of high and low cell density regions, by counting cell nuclei within the neointima that forms around the wire implant. Cross sections of each wire are examined with a JEOL scanning electron microscope. This provides backscattered electron images, which differentiates remaining zinc, corrosion product, tissue, and epoxy in each sample. These images allow us to assess corrosion behavior and quantify penetration rates for each alloy composition evaluated. "

Results and Discussion:

The biological response to the three magnesium concentrations was evaluated from histological images collected at 6 and 11-month time points. The host response was generally similar to what we recently reported for pure zinc, although a slightly higher presence of inflammatory cell infiltrates lead in some cases to a slightly greater degree of neointimal activation or arterial constriction. There appears to be a trend of slightly worsening biocompatibility with increasing Mg content, consisting of intimal activation propagating away from the implant, decellularized regions of neointimal tissue, toxic regions near the original endothelium of the artery, and some degree of arterial constriction. In contrast, the neointima that formed around pure zinc implants was generally restricted to the implant vicinity and neither overt toxicity nor arterial constriction was detected.

12. Tungsten Disulfide as a Counter Electrode in Dye-Sensitized Solar Cells

Student Presenter: Simon Eddy, Materials Science & Engineering
Faculty Advisor: Yun Han Hu, Materials Science & Engineering

Introduction:

With climate change becoming a major concern in today's society, further research in alternative energy is crucial. Among the various renewable energy sources, solar energy is unarguably the largest source with potential to be scaled up to meet our energy needs. The dye-sensitized solar cell (DSSC) is a promising third generation photovoltaic device that can convert solar energy to electrical energy. It is composed of three main parts; the dye-sensitized photo electrode, an electrolyte solution, and a counter electrode (CE).

Materials and Methods:

Currently, the standard CE for DSSCs is a platinum (Pt)-coated conductive glass. This is due to its high catalytic activity and excellent conductivity. However, the limited supply and high cost of Pt limit its practical applications. Therefore, it is necessary to develop Pt-free counter electrodes for DSSCs. In this research, Tungsten Disulfide (WS2), a highly lubricous and temperature resistant material, has been explored as CE materials for DSSCs. Furthermore, mechanical and thermal processing techniques such as ball-milling and heat treatment were employed to increase its electrical conductivity and catalytic activity.

Results and Discussion:

A power conversion efficiency of 2.59% was achieved through multiple trials, indicating that WS2 is a good candidate to replace the Pt CE in DSSCs.

13. Synthesis of a Fructopyranose Mimic as a Carbohydrate Probe for Fructose Transporters

Student Presenter: Alexis Ferrier , Chemistry
Faculty Advisor: Dr. Marina Tanasova, Department of Chemistry

Introduction:

The goal of the project is to synthesize stable fructopyranose mimics as tools to distinguish cancer from normal cells on the basis of fructose uptake efficiency. Stable fructose mimics are needed to eliminate from the account multiple conformational isomers that represent fructose in aqueous media, and focus on the interaction of a major fructose conformer – fructopyranose – with fructose transporters. They also provide the possibility to alter the stereochemistry of fructose hydroxyls to derive structure-affinity relationships revealing key interactions to target fructose transport.

Materials and Methods:

A large variety of organic synthetic techniques were used. Inert (air-free) and anhydrous conditions were necessary for many of the synthetic steps. Anhydrous conditions were achieved by the use of flame-dried glassware and oven baked needles under atmosphere of dry argon, and applying anhydrous solvents. Reactions requiring thermal conditions were conducted in a fume hood and heated to the various temperatures using an oil bath. For sensitive reactions involving organometallic reagents, a cooler was used to reach cryogenic conditions. The reaction progress was checked using Thin-Layer Chromatography (TLC) with co-spotting the starting material against the reaction material. If the reaction was determined complete i.e. little to no starting material was left the reaction was stopped. Most reaction work-ups were done using extractions, distillations – both regular and vacuum – and filtrations. Purification was performed using crystallization, distillation and column chromatography techniques. The purity of the products of each step were checked using TLC, 1H and 13C Nuclear Magnetic Resonance Spectroscopy. The multiplicity of carbon atoms was determined by DEPT-135 experiment if necessary. Mass Spectroscopy using electrospray ionization was used to determine the molecular weight.

Results and Discussion:

Synthetic approaches to fully functionalized pyranoses are challenged by the necessity to install multiple chiral centers and perform chemical transformations on highly functionalized building blocks. The original approach to synthesize fructopyranose mimics was based on using the allyl substitution reactions that allowed for a consecutive installment of hydroxyls in a well-controlled stereoselective manner. Some synthetic steps presented significant challenge including low percent yields, necessitating development of an alternative, more efficient approach to functionalized pyranoses. The alternative approach using amino acid as a source of chirality proceeded with good to moderate yields until the crucial tandem ester reduction/Grignard reaction step to produce a cis-diol. During this step, a decomposition of the substrate occurred. Despite multiple attempts to improve this transformation, no further advancement to the target fructopyranose via this alternative route was possible. The newest, more successful approach to synthesize the mimic relies on classical methods to install and control chirality of hydroxyls.

14. The Effects of Uncertain Labels on Damage Assessment in Remotely Sensed Images

Student Presenter: Brian Flanagan, Computer Engineering
Faculty Advisor: Dr. Timothy Havens, Electrical and Computer Engineering

Introduction:

In the event of a natural disaster, proper decision-making is of great importance. The ability of emergency teams to respond quickly and correctly to a given disaster greatly reduces the resulting financial and human cost of that event. A reliable assessment of the damage becomes invaluable when attempting to lower these costs after an emergency. This project's goal is to develop a fuzzy classifier that will quickly, accurately, and automatically classify areas of likely damage based on remotely sensed images of the disaster, while simultaneously learning the characteristics of the damage in the images for future use.

Materials and Methods:

To begin the project, I created a program in MATLAB, which used data that has already been generated from multiple remotely sensed images at various segmentation levels (from small segments to larger segments), to train a crisp Support Vector Machine (SVM). I used cross validation, feature selection, and parameter optimization in order to create the most accurate classifier attainable. Once the crisp classifier was created and producing valid results, I created a soft-label classifier. Using the crisp classifier as a baseline, I later measured the results of the fuzzy SVM. The same data was used for both types of classifiers, but the class labels for the soft SVM were not binary; instead, they had probabilities associated with them that corresponded to the mixed labels in the image segment. Once again, cross validation was used to attain the best possible soft classifier and to assess real-world performance. When both types of classifiers were producing satisfying results, the process of comparing them began. Receiving Operating Characteristic (ROC) curves were used to assess the comparison of the classifiers. Finally, I examined the classification results to show what merit there is to using classifiers that can account for soft labels to classify remotely sensed natural disaster images.

Results and Discussion:

My hypothesis for this project was that an SVM with fuzzy logic applied to it would classify better than a crisp SVM, as it would be able to more appropriately account for the uncertainty in the training image segments. After creating a crisp SVM and a fuzzy SVM, each using a linear kernel function, I ran a validation test 300 times at each segmentation level and recorded the average area under the ROC. Both classifiers performed well, and the fuzzy SVM did produce marginally better classification results, but not enough to be statistically significant. Through extensive testing it would appear at this point that the inclusion of uncertain labels in the training data does not necessarily improve classification results. For the remainder of the semester I will continue my attempts to improve the classifications produced by both the fuzzy and crisp SVMs. I will attempt to replace the linear kernel function used in the SVMs with a radial basis function kernel, with the hope that classification results will improve once it is optimized. This change may show evidence that the fuzzy SVM is able to outperform the crisp SVM.

DeVlieg Foundation

15. Characterization of Electrospun Nanofiber Scaffold for Wound Healing Applications

Student Presenter: Meghan Friske, Biomedical & Electrical Engineering
Faculty Advisor: Dr. Smitha Rao, Biomedical Engineering Department

Introduction:

Tissue scaffold engineering is an active field of research for drug delivery, cell behavior studies, constructive surgery and regenerative medicine. Scaffolds are engineered to match tissue properties (tensile strength, elasticity, etc.) using techniques such as electrospinning of polymers in solution. Often these synthetic polymer networks have the required mechanical properties, but lack biocompatibility, creating an inflammatory host response. In this work, the biocompatibility and wound healing properties of nanofiber scaffolds made of biodegradable polymers such as polyvinylidene difluoride (PVDF), polyaniline (PANI) and polycaprolactone (PCL) was determined.

Materials and Methods:

The biocompatibility of the nanofiber scaffolds was determined by analyzing cardiac and skin cell migration, growth, and proliferation through direct cell seeding. Rat cardiomyoblasts, H9c2 (CRL-1446, ATCC), and human skin cells, Detroit 551 (CCL-110, ATTC), were cultured and seeded onto different types of nanofibers with a cell seeding density of 20,000 cells each. These fiber samples were fixed in 4% paraformaldehyde after 1, 2, 3, and 7 days and stained with DAPI/Alexa Fluor for fluorescence imaging. Samples were dried using hexamethyldisilazane (HMDS) and then sputter coated with a 5nm thick layer of Au-Pd before visualizing using the FESEM. Similarly, samples with cells were treated with 10 µM Bromodeoxyuridine (BrDU) and stained with secondary antibodies for appropriate duration and fixed for fluorescence imaging. Wound healing properties of the nanofiber scaffolds were determined through a scratch wound assay. The cells were seeded onto the fibers and after 24 hours, a scratch was created using an innoculation loop. After a period of 6, 12, and 24 hours, the fibers were fixed in 4% PFA and stained with DAPI/Alexa Fluor for fluorescence imaging.

Results and Discussion:

PCL had some cell attachment and growth after 1, 2 and 3 days but very little after day 7. BrdU staining indicated that the cells did not proliferate on the PCL fibers. PCL-PVDF had good cell attachment and proliferation from day 1 to day 7 and BrdU staining supports this claim. The addition of PVDF β-phase crystalline structure gives nanofibers piezoelectric properties creating an environment more suitable for cell differentiation. Despite this, both PCL and PCL-PVDF fibers had clumping of cells. PCL-PVDF-PANI had the best cell attachment after 7 days and the cells appeared to embed into the nanofibers and penetrate into the layers. BrdU staining indicated that cell proliferation was the most abundant in these fiber scaffolds. The cells were also more aligned on these scaffolds due to the addition of PANI. Scratch wound assays show that PCL-PVDF-PANI create an environment that is best suited for wound healing. These findings indicated that the nanofiber scaffolds can potentially be used as cardiac patches, skin grafts, or in other wound healing applications. By analyzing the electrical characteristics of the fiber, the research can be extended to other areas including neural tissue engineering.

PHFoundation

16. Structural Health Monitoring using UAV's and Kinect Sensors

Student Presenter: Samuel Gaines, Civil Engineering
Faculty Advisor: Hyungchul Yoon, Civil Engineering

Introduction:

Finding methods of inspecting aging civil structures in order to assess structural damage and need for repairs is important in today's world. This research addresses this issue by using a Microsoft Kinect sensor to establish a more cost effective method for evaluation. The Kinect sensor has both a color RGB and a depth infrared sensor providing accuracy at consumer prices, making such structural health monitoring more accessible and cheaper in the future. A UAV was also implemented to give the Kinect Sensor more mobility and range.

Materials and Methods:

Research began with the understanding of how computer vision programing interfaced with the Kinect sensor and Matlab, the chosen programming language. A combination of information feeds from the two cameras on the Kinect allowed the construction of a 3D point cloud model that gave (x, y, z) coordinates for every point in the field of view. Once we found coordinates for every point in every frame of a video, we used computer vision systems to detect and track the points throughout the video. Using measured displacement, identification of the system structure was done with algorithms such as ERA. UAV implementation then allows for more mobile and fluid data gathering. In order to differentiate UAV movement from structural movement, a known stationary point is tracked whose motion is subtracted from that of the structure's.

Results and Discussion:

Testing of the accuracy of the Kinect sensor confirmed that using a consumer grade camera was a viable method of structural health monitoring and further computer vision applications. Finding this displacement can be used to localize the damages in a structure visualized with the 3D point cloud.

DeVlieg Foundation

17. Building-to-Grid Predictive Power Flow Control for Demand Response and Demand Flexibility Programs

Student Presenter: Drew Hanover, Mechanical Engineering
Faculty Advisor: Mahdi Shahbakhti, Mechanical Engineering-Engineering Mechanics

Introduction:

Rapid penetration of renewable energies such as solar and wind power onto the power grid has created a shift in how electricity is generated. Mismatches in power demand and power generation due to rapid changes in weather conditions can drastically impact the electricity market in a volatile manner, causing large price fluctuations that are inevitably forced upon the consumer. This research examines the feasibility of Demand Response energy programs where bi-directional communication between commercial buildings and the electric power grid can offer large savings for both the consumer and supplier of energy by altering the HVAC control strategy. Demand response programs can help to stabilize the power grid while also offering significant savings on electricity costs.

Materials and Methods:

A control framework for HVAC systems within commercial buildings can be developed using Model Predictive Control (MPC) to modify HVAC operation from traditional rule-based control to an optimized control strategy used to reduce energy consumption. A mathematical model for photovoltaic (PV) panels is re-created based on a National Renewable Energy Laboratory publication. This model is used to predict solar power generation based on climate data for Houghton, MI. The model is validated using solar power data from the Keweenaw Research Center's solar array. In addition, a thermal model for a commercial building is developed to predict temperature and energy dynamics within the building. The thermal model is created using a technique known as Resistance Capacitance (RC) modeling. RC modeling is used to model heat transfer between zones within a building. The RC building model is validated using experimental data from the Lakeshore Center building at Michigan Technological University.

Results and Discussion:

Combining MPC with the thermal and PV models, DR can be used to control power flows to and from the grid to help stabilize the grid and provide the consumer with compensation. The following research examines implementation of the optimization control framework into two different configuration topologies for a commercial building. Our results show that the proposed control framework can significantly reduce energy consumption and peak load contribution associated with PV penetration onto the grid. The DR service does not alter the building climate in a noticeable way, and can offer electricity consumption savings of 26% and improvement on grid ramp up and ramp down rates by 30% and 14.5% respectively.

18. Investigation into the Free Radical Scavenging Activity of Novel Nitroxide Derivatives

Student Presenter: Jackie Harris, Chemical Engineering
Faculty Advisor: Dr. Lanrong Bi, Chemistry

Introduction:

I/R injury represents tissue damage associated with the return of blood supply following an ischemic period that can trigger a systemic inflammatory response leading to cellular damage and even organ failure. It is widely felt that ROS and polymorphonuclear leukocytes play important roles in mediating I/R injury. Accordingly, antioxidant supplementation and anti-inflammatory agents may represent a rational therapeutic approach in alleviating I/R injury. Studies indicate that nitroxides can attenuate oxidative damage in various I/R experimental models. These nitroxide protective effects are attributed to their antioxidant capacities.

Materials and Methods:

The sample compounds evaluated were C13H2102, C9H17N4O, and C10H18NO3. The compounds were tested at three different solution concentrations (125 µM, 62.5 µM, and 32 µM) in 50 mL dimethyl sulfoxide (DMSO). Each of the prepared sample compound solutions were mixed with 500 µL linoleic acid emulsion in 0.02 M potassium phosphate buffer and incubated in a warm water bath at 37°C for 24 hours. Aliquots of 0.1 mL of each sample were taken following incubation and sequentially added to prepared solutions of ethanol, ammonium thiocyanate, and ferrous chloride in hydrogen chloride (HCl). Each sample was analyzed using a UV-vis spectrometer with the prepared ethanol solution added to each sample used for the blank sample, and the prepared linoleic acid emulsion was used as the control sample. The above procedure was performed in triplicates for each solution to show the reliability of each prepared sample being tested, which was compared using selected peaks showing absorption and wavelength for each UV-vis spectrum.

Results and Discussion:

The UV-vis Spectrometer results for each concentration had possible outlier data during trial 1 for each compound; however, the overall trials for each sample showed the results were reproducible. The average LPI% data showed the best antioxidant activity was for 125 µM of C10H18NO3 at 62.96% ± 1.71. The lowest average LPI% was 60.99 ± 0.13, and subsequent lowest antioxidant activity, was for 32.5 µM of C10H18NO3. Sample compound C10H18NO3 showed the highest and lowest LPI%, but overall the 125 µM sample was the best of all sample compounds for LPI% determination; therefore, this sample compound is the one being recommended for future research of these compounds. All compound trials were very close in LPI%, which means that each compound can be considered a good free radical scavenger. The overproduction of reactive oxygen species resulting from mitochondrial oxidative damage can lead to multiple forms of disease including ischemia/reperfusion injury. The development of lead compounds exhibiting free radical scavenging activity can help protect the mitochondria and act as a therapeutic method of treatment. The compounds each showed good free radical scavenging activity, and are recommended to continue working with in developing a therapeutic treatment with compound C10H18NO3 showing the most promise.

19. Finding Structure in Data

Student Presenter: Madison Heeringa, Mathematics: Actuarial Science
Faculty Advisor: Benjamin Ong, Department of Mathematical Sciences

Introduction:

Multi-scale principal component analysis (PCA) is a recent development that can be used to find structure in large data sets. In standard PCA, one uses the singular value decomposition to find a hyperplane that approximates the data. In multi-scale PCA, the idea is to systematically correct the hyperplane approximations at different levels/resolutions by repeatedly using the singular value decomposition to find hyperplanes which approximate the error between the approximations and the original data. The focus of this project was to learn about and understand PCA and multi-scale PCA.

Materials and Methods:

For two-dimensional data (the standard x-y plane), a hyperplane is simply a standard regression line. Using MATLAB, we construct multiple scale approximations of discrete data generated from the function, y = sin6x. We used the polyfit function to determine a line of best fit at each scale which approximates the error between the original data and the piecewise-linear approximation. To find a hyperplane approximation in higher dimensions, the singular value decomposition must now be used to find a hyperplane of best fit. We tested the multiscale algorithms on data generated from the function f(x,y,z) = y-sin6x.

Results and Discussion:

This research is ongoing, and will eventually be used to classify land and canopy cover in satellite images, which can subsequently be used for water resource management.

20. Development of a Novel Injectable Nitric Oxide Releasing Fibrin Microgel Composite Hydrogel for Tendon Repair

Student Presenter: Carly Joseph, Biomedical Engineering
Faculty Advisor: Dr. Rupak Rajachar, Biomedical Engineering

Introduction:

Tendon injuries can be acute or chronic, and in both cases can lead to fiber degeneration and pain in injured tissues. Invasive surgical techniques are often used in their repair. A minimally invasive approach to the stabilization and healing of tendon injuries may be achieved through an injectable poly (ethylene) glycol (PEG)-fibrinogen hydrogel incorporating nitric oxide (NO) releasing fibrin microparticles with beneficial wound healing and cell adhesive properties. The aim of this work is to fabricate NO releasing microparticles and incorporate them into a PEG-fibrinogen hydrogel for use in an injectable tendon repair system.

Materials and Methods:

Microparticles were generated using a simple emulsion polymerization process through which particle size distribution can be controlled using fluid shear stresses generated via stirring. S-Nitroso-N-acetyl-D-penicillamine (SNAP) was synthesized and used as the NO donor for this work. Fibrinogen blended with SNAP was injected dropwise into a stirring olive oil bath. Thrombin was injected immediately afterwards. The emulsion was mixed at speeds of 750, 1000, and 1500 rpm. Particles were imaged and their diameters and size distributions were quantified. NO release from the particles was evaluated in real-time through chemiluminescent analysis using a nitric oxide analyzer. The capacity for NO release was validated via photolytic degradation with a 470 nm LED. Microparticles were then incorporated into a PEG-fibrinogen hydrogel and the NO release was measured as previously described. Compressive and rheological properties were also determined for the composite hydrogels. Biocompatibility was assessed through live/dead staining and a MTT assay. PEG-fibrinogen hydrogels without particles served as controls.

Results and Discussion:

The mean particle diameters ranged from 78–193 μm. Samples prepared at 750 and 1500 rpm were characterized by excessive debris and irregular shaped particles. The 1000 rpm samples exhibited minimal debris, spherical character, and a narrow size distribution, and were used throughout the remainder of this work. NO release studies show consistent, controlled release for the individual particles as well as for the composite hydrogels. Mechanical data sugests that the microgels are similar in character to their particle free analogues. Rheometric data shows both storage and loss moduli at comparable levels to the control samples. Fibroblasts cultured onto the composites maintained viability and were non-cytotoxic as measured by the MTT assay.

21. Understanding Lake Superior Warming through Observational Data and Model Results

Student Presenter: Ryan Kibler, Environmental Engineering
Faculty Advisor: Dr. Pengfei Xue, Civil and Environmental Engineering

Introduction:

Despite vast research regarding the Great Lakes region, consistent hydrodynamic modeling of the Great Lakes has still not been perfected. Over the past decade, studies have been published investigating the impacts of climate change on Lake Superior. Several studies have focused on summer warming and have concluded that Lake Superior's summer surface water temperature is warming at a rate twice as fast the surrounding region's air temperature over the past 30 years. However, there has been far less research on the impacts of climate change on winter warming partly due to the lack of observations.

Materials and Methods:

In this study, several data sets and model results are utilized to examine the changing heat content of Lake Superior.

Results and Discussion:

Results show that the winter warming is comparable to the summer in terms of heat content, suggesting it is a more representative method to define warming in Lake Superior.

22. Sulfenamide Form of Omeprazole in Interaction with the Primary Amino Acid Sites of H+/K+ ATPase as Investigated at Electronic Structure Level

Student Presenter: Emily Lilla, Chemistry
Faculty Advisor: Loredana Valenzano, Chemistry

Introduction:

Omeprazole (Prilosec®) is the first medication that treats gastroesophageal reflux disease (GERD), and serve as proton pump inhibitors (PPI). It inhibits the enzymes CYP2C19 and CYP3A4, and prevents the final step of acid production and basal and stimulated acid secretion. Omeprazole must be converted into the active drug in the stomach acid, turning it into sulphenamide. The molecule then undergoes covalent bonding on cysteine 813 and 892 in the luminal domain of the H+/K+ ATPase system in gastric parietal cells, and they are identified as the primary, and secondary binding site, respectively.

Materials and Methods:

We used Density Functional Theory (DFT) to determine the equilibrium geometries for each molecule using different levels of theory. Atoms were described within the linear combination of atomic orbitals (LCAO) approach as implemented in the Gaussian09 program. After a preliminary exploration of the relative stability of the two isomers omeprazole and esomeprazole, this work addresses at quantum chemical level the complexation energies of the sulfenamide species originated from omeprazole with respects to cys-813 and cys-892. Geometry relaxation, and frequency calculations were run at PBE/6-311G(d,p) level of theory in vacuum, water, and hydrochloric acid. Single point energy calculations were then performed at 6-311++G(d,p) and 6-311++G(2d,2p) level. The two sequence of amino acids were built following a step-by-step procedure by adding one residue at the time around the two cysteines binding sites. In both cases, the assembly procedure was completed after chains of six amino acids were created. Calculations were then ran for all the individual segments with and without the presence of sulphenamide.

Results and Discussion:

PBE/6-311G(d,p) results obtained in vacuum, aqueous, and acidic environment on the complexation energies have shown to have a consistent trend. These results are the starting point for addressing the interaction between omeprazole and the biological activation sites. As such, this work is unique, and it has the following outcomes: (i) it provides a comparison between the complexation energies of the two major binding cysteine sites; (ii) it allows for identifying the influence of the H+/K+ ATPase chemical environment; (iii) it provides a template for other similar studies conducted at electronic structure level.

23. Changes in Tropospheric Ozone Formation with a Reduction in PM Over China

Student Presenter: Jeremy Luebke, Environmental Engineering
Faculty Advisor: Dr. Shiliang Wu, Civil & Environmental Engineering

Introduction:

"There have been serious concerns on air pollution in China, especially on hazardous levels of particulate matter (PM) in the air, which leads to significant efforts on reducing anthropogenic emissions of PM. On the other hand, there are complicated interactions between PM and ozone, another major air pollutant. For example, solar radiation which is critical to driving ozone production can be reduced by atmospheric PM. This implies that, with the cleanup of atmospheric PM, atmospheric ozone formation could be enhanced, but the issue has never been explored before."

Materials and Methods:

"We use a well-established atmospheric chemistry model, GEOS-Chem, in this study to examine the potential impacts on atmospheric ozone from changes in PM. GEOS-Chem is a global 3-D chemical transport model (CTM) for atmospheric composition driven by meteorological input from the Goddard Earth Observing System (GEOS) of the NASA Global Modeling and Assimilation Office. A baseline control run was first conducted to simulate the present-day air quality over China. A series of sensitivity simulations were carried out where the atmospheric PM is decreased by 25%,50%,75%, and 100% respectively. Through these sensitivity simulations, we would be able to derive the impacts on atmospheric ozone from changes in PM."

Results and Discussion:

Our model simulations confirm that the tropospheric ozone would increase with decreasing PM. It was also discovered that the increase in tropospheric ozone does follow a linear relationship with decrease in PM. For example, in May when PM is decreased by 50%, tropospheric ozone levels increased up to 3% of normal levels. In May, when PM was decreased by 100%, tropospheric ozone levels increased up to 6% in the same areas over China. This implies that, although cleaning up of PM pollution over China are desired, it could also lead to increases in ozone pollution unless further actions are taken.

24. What Do You Think Before You Fall?

Student Presenter: Hannah Maat, Exercise Science
Faculty Advisor: Dr. Tejin Yoon, Human Neuromechanics Laboratory

Introduction:

The prefrontal cortex (PFC) plays an important role in cognitive control, motor planning, and execution of movement. Although the biomechanics, physiology, and psychology of the sport of rock climbing has been studied, there is no published research examining PFC activation during a climbing specific task. The purpose of this study is to examine cortical activation in the PFC during a sustain hang until failure.

Materials and Methods:

This study will seek 15 volunteers. Participants will be asked to hang from a rock climbing training device known as a hangboard. This is equipped with a variety of climbing-specific holds to grip with the hands. Participants will hang until they can no longer maintain themselves on the holds. During this hanging task participants will wear a 16 channel fNIRS device on their forehead which will monitor their PFC activation. Activation will be quantified as changes in oxygenated and deoxygenated hemoglobin in the PFC.

Results and Discussion:

Although fNIRS has been used to explore an assortment of sports and tasks, it has not yet been used to study hemodynamics of the brain. We hope to find specific areas and patterns of activation in the PFC during this physically and mentally demanding task.

25. Predicting the Rejection Efficiencies of Toxicologically Relevant Organics in Reverse Osmosis of Wastewater Reclamation Processes

Student Presenter: Mary Kate Mitchell, Chemical Engineering
Faculty Advisor: Dr. Daisuke Minakata, Environmental Engineering

Introduction:

As water scarcity becomes more prevalent, many communities will turn to direct potable reuse (DPR) to help augment their water supply. Concerns about the presence of trace level organic compounds in wastewater effluent prompted the need for better understanding of typical rejections from the most dominant technology in DPR, reverse osmosis (RO). We calculated the mass transfer coefficients of salt and water based on commercially available salt rejection data of various RO membranes and combined with physicochemical properties of organics, developed a quantitative structure activity (QSAR) model for the prediction of rejection efficiencies of a wide range of organics.

Materials and Methods:

This study focuses on eight popular polyamide RO membranes from various manufacturers which include Dow Filmtech BW30HR, Dow Filmtech NF270, Dow Filmtech SW30XHR, GE AG LF, GE AP, Hydranautics ESPA2-LD, Toray TM800M, and Toray TMGD. Using values from manufacturer data sheets and RO equations for rejection, concentration, and flux, the mass transfer coefficients for salt and water were calculated. The data was plotted and a trend was obtained. Next, we selected about 110 toxicologically relevant organics that contain various functional groups and calculated their physicochemical properties, such as Kow, solubility, molecular volume and weight. We developed QSARs that relate those properties with the mass transfer coefficients of organics obtained by benchtop experiments using genetic algorithm. Finally, we develop a process model by including the operational RO parameters such as applied pressure, feed concentration of organics, and flow rate.

Results and Discussion:

The salt and water mass transfer coefficients for the RO membranes were found to have a linear relationship on a log-log graph, which is useful for characterizing the membrane in use based on only information that is readily available from membrane datasheets. The experimentally determined mass transfer coefficients for the organics by a various RO membranes and at 3 different applied pressures were linearly correlated with physiochemical properties of organics using genetic algorithm. A comprehensive model that predicts organic removal efficiency will then be available for wastewater treatment plants utilizing DPR. This model will be valuable due to its inclusive nature of many categories of pathogens and emerging chemicals and several types of RO membranes. Knowledge of RO removal efficiencies will reveal potential public health risks and allow the risks to be mitigated.

DeVlieg Foundation

26. The Geminga Pulsar Wind Nebula and the Positron Excess

Student Presenter: Kelci Mohrman, Physics
Faculty Advisor: Dr. Petra Huentemeyer, Department of Physics

Introduction:

Geminga (PSR J0633+1746) is a rotating neutron star, called a pulsar, located in the direction of the constellation Gemini. Surrounding the pulsar itself is a pulsar wind nebula (PWN), which accelerates particles to high energies and emits constant gamma radiation. It has been suggested that the particles accelerated by the Geminga PWN could explain the observed excess in the locally measured positron flux, though it was also proposed that this anomalous overabundance of positrons could be a consequence of the annihilation or decay of dark matter.

Materials and Methods:

The purpose of this project is to identify and model the gamma-ray emission of the Geminga PWN in GeV energies using data from the Fermi Space Telescope in order to determine the potential contribution to the local electron and positron flux. The gamma-ray emission resulting from the particles accelerated by the nebula travels to earth without being deflected by magnetic fields; consequently, gamma rays represent the best messengers to probe the charged particles ejected by the pulsar and accelerated by the surrounding nebula. The central piece of the analysis is a maximum likelihood fit, which establishes the significance of a source's variance above its surroundings by fitting a combined extended source and background model to the data.

Results and Discussion:

The PWN is modeled with a diffusion model, which will allow us to determine the size of the electron and positron cloud diffusing from the nebula and consequently the contribution to the electron and positron flux, therefore potentially establishing whether the PWN explanation of the locally measured positron excess can be substantiated.

27. An Experimental Investigation of the Role of Spatial Working Memory in Age-Related Declines in Motor Learning

Student Presenter: Madelyn Morley, Exercise Science
Faculty Advisor: Kevin Trewartha, Psychology

Introduction:

Motor learning requires two memory components: a fast, rapidly adapting component and a slow, gradual adapting component. Research has shown that age-related declines in working memory are associated with impairments in the fast component of motor learning. However, the precise nature of the working memory mechanisms underlying age-related changes in the fast process for motor learning is unclear. The current project was designed to investigate whether spatial working memory resources in particular, underlie age-related declines in the fast component by manipulating spatial working memory load during a motor learning task and comparing performance between younger and older adults.

Materials and Methods:

A group of older adults aged 60 to 85, and a group of younger adults aged 18 to 30 years old were recruited to perform a variant of a well-known sensorimotor adaptation task. Participants made out and back movements to four visual targets arranged around the periphery of a home position while grasping a handle attached to a robot that generates unusual movement-dependent forces at the handle (KINARM, BKIN Technologies). Although the load initially perturbs hand movement, people gradually adapt by producing forces that counteract the load. Participants from each age group were randomly assigned to a high or low working memory load condition. In the high load condition, the order in which the targets were presented was randomized, whereas in the low load condition the targets appeared in a repeating four-target sequence. Participants also performed a cognitive battery including a verbal paired-associate memory task, a spatial working memory task, and an implicit memory task. This battery allowed us to independently evaluate the correlations between the fast process for motor learning and spatial, and associative working memory resources, respectively, in younger and older adults.

Results and Discussion:

Within each age group, one subgroup of participants learned the motor skill while reaching to targets presented in a random order, whereas a second sub-group reached for targets in a repeating four-target sequence. These groups were compared to test the hypothesis that older adults were disproportionately affected by the high working memory load condition compared to younger adults. Correlations between each cognitive test and the rate of motor learning were calculated for each age group to test the hypothesis that the fast process is more related to spatial than associative working memory, and that the correlation is stronger for older than younger adults. Combined, the current data contributed to our understanding of the memory mechanisms underlying motor learning, and the nature of age-related changes in those memory processes in later adulthood.

PHFoundation

28.The Effects of Nano-Sized Particles in Ultrahigh Carbon Steels

Student Presenter: Charles Newlin, Materials Science and Engineering
Faculty Advisor: Edward A Laitila, Materials Science and Engineering

Introduction:

"The goal of the research is to further the application use of iron carbon steel alloys consisting of ultrahigh carbon (UHC) steels ranging from 1.0-2.0wt% carbon. Today, UHC steels are restricted to cutting tools due to their characteristically high hardness. However, the hardness of a material can be manipulated using the Hall-Petch relationship. Under the Hall-Petch relationship materials will have a greater resistance to permanently deform with smaller and smaller grain sizes and results in a harder material. However, upon reaching critical grain sizes of 10 nm, a material will exhibit the reverse Hall-Petch relationship, meaning a material will be more susceptible to permanent deformation with smaller and smaller grain sizes and will result in a softer material."

Materials and Methods:

The 25 Grams of iron-carbon powder of 1.5 wt% carbon ground to nanometer sized particles was consolidated by two material processes: cold isostatic pressure commonly referred as CIP and hot isostatic pressure commonly referred as HIP. The cold isostatic pressure process was undertaken with 35,000 psi at room temperature with the goal to convert the fine iron-carbon powder into a solid form referred to as green state. The sample material was then wrapped in tantalum foil and placed in a copper canister. Prior to the HIP process, the copper canister is vacuum degassed and welded shut. The HIP process was undertaken at 25,000 psi at 950 degrees Celsius for two hours under argon gas. The HIP process is followed by a cooling rate of 25 degrees Celsius per minute. Following the consolidation of the UHCS sample, the hardness of the material is measured using a Rockwell B tester and a Vickers Microhardness Indenter. The field emission scanning electron microscope was then used to measure the average grain size in order to relate the overall hardness of the UHC steels to the average grain size of the material.

Results and Discussion:

The CIP and HIP processes are crucial in restricting the size of the grains present in a material. The CIP process is used to increase the overall density of the fine powder. Whereas the HIP process fuses the particles together without melting the overall material. This is similar to ice cubes solidifying together in cold water. For example, if there were two glasses of water and in one glass normal sized ice cubes from an ice cube tray were placed the glass, and in the second glass, the ice cubes were broken in half before being added. In both glasses, the overall volume of ice would be the same but the average cube size would be different. The ice chunk made with smaller cube sizes would be harder than the other ice chunk. Manipulating the size of ice cubes or metallic grains is crucial in modifying the overall hardness of a material. Modifying of the characteristically high hardness of UHC steels is crucial in opening the door for new applications of UHC steels mainly in the realm of structural engineering.

29. Linear Traverse Design Project for Research Applications in the Cloud Chamber

Student Presenter: Thomas Page, Mechanical Engineering
Faculty Advisor: Dave Ciochetto, Physics

Introduction:

Due to the stationary nature of existing data collection methods inside the atmospheric cloud test chamber, a linear traverse was desired by researchers to allow measurements along one axis. The current measurement model allows only for a basic idea of the conditions inside the cloud chamber, and the ability to move the measurement instruments remotely gives a more detail picture of the processes inside.

Materials and Methods:

The project was an iterative building process that required many physical parts as well as 3D modelling software to design and improve each iteration. Although not every piece that was used made it into the final project, each contributed to the overall design.

Results and Discussion:

The physical hardware consisting of the carriage to hold the instruments, the linear bar that the carriage moves along, the drive motor and the pressure case for the motor, and the drive belt were all finished. Work was started on the electronic control system, but not finished due to limitations.

30. Macroinvertebrates in Hammel Creek

Student Presenter: Emily Praznik, Environmental Engineering
Faculty Advisor: Dr. Noel Urban, Civil and Environmental Engineering

Introduction:

In the nineteenth and twentieth centuries, operating copper mines throughout the Keweenaw discharged toxic substances into nearby streams, destroying the habitats and killing wildlife. In particular, during operation (1873-1968) of the Osceola Mines near Calumet in the Upper Peninsula of Michigan dewatering of the mineshafts resulted in pumping brine into Hammell Creek. Now that the mines are no longer in operation, the stream has begun to recover. However, water with high salt and metal content still flows freely out of the shaft of Osceola #4, and this discharge represents a large fraction of the water flow in Hammell Creek. My research quantified macroinvertebrate populations in Hammell Creek downstream of mine discharge to determine over what distance the stream invertebrates are negatively impacted.

Materials and Methods:

This project included initial reconnaissance of the area, identifying suitable sampling locations along the stream, collecting and enumerating macroinvertebrates, and analyzing the data. I first reviewed results of research previously done on the stream. Next, seven sampling sites were chosen along the stream. Data collected from each site included conductivity, dissolved oxygen, and temperature. Macroinvertebrates were collected from each site by scrubbing rocks in a set area into a collecting net. A PVC square was used to ensure the same size sample was taken at each site. Macroinvertebrates were stored in denatured alcohol until they were identified in the lab. Additional water samples were also taken from each site in the stream and sent to a lab to identify trace metal concentrations.

Results and Discussion:

The composition of the macroinvertebrate assemblage changed greatly downstream from the mine discharge. The first three sampling locations were dominated by pollution tolerant taxa (midges, worms), while pollution-sensitive taxa were abundant at stations farther from the mine. While the total abundance of organisms was not greatly reduced near the mine, the types of organisms were restricted to those tolerant of pollutants.

31. Synergistic Effect of Graphene-Oxide-Doping and Microwave-Curing on Mechanical Strength of Cement

Student Presenter: Hao Qin, Material Science
Faculty Advisor: Yun Hang Hu, Materials Science & Engineering

Introduction:

Cement is a main component of concrete with nano-structures and multi-phases. As an important engineering material, concrete cement possesses an excellent compression strength. However, micro-cracks, which appear during the deformation processing of cementation matrices, keep growing and thus decrease its compression strength. Various types of fibers, such as steel fibers, glass fibers, and polypropylene fibers, are used to inhibit the cracks.The fiber's mechanical properties and geometry as well as the curing methods will determine how the cement will be strengthened. The mechanical properties of cement also relate to matrices. In this research, graphene-oxide used as a fiber to enhance the strength of cement.

Materials and Methods:

The type of cement used in this research was Portland cement type II (No.1124). The ratio of Portland cement, sand, water and polycarboxylate superplasticizer (PC) solution was 1: 3: 0.3: 0.1. Different percentages of GO were added depend on changing of sample mass. Polycarboxylate, cement, sand, water, and graphene oxide solution were mixed together and kept stirring until fitted into the mold. The average size of samples was 14 in thickness and 14 in width with 28 in length. All samples were placed in the mold for 24 hours. After the ceramic structure initiated then all the sample were removed out from molds and covered with wet sponges. Samples were tested in 5 different periods, 3, 5, 10, 14, and 28 days, respectively. All compression tests were carried out by Intro 2406 mechanical testing machine.

Results and Discussion:

The compression strength of plain cement is 14.3 MPa. The strength can be enhanced to 32.4 MPa by GO-doping and microwave curing, which is an increase of 127%. The highest compression strength (32.4 MPa), which was achieved by combining GO-doping and microwave curing, is 127% higher than that without GO-doping and microwave curing. Furthermore, XRD and, FTIR, and FESEM characterizations revealed that such a significant enhancement was due to the acceleration of hydration process of cement by GO-doping and microwave curing.

32. Covalently Bonded Collagen Coating on PDMS Improved Human Mesenchymal Stem Cell Sheet

Student Presenter: David Ross, Biomedical Engineering
Faculty Advisor: Feng Zhao, Biomedical Engineering

Introduction:

Human Mesenchymal Stem Cells (hMSCs) can be used in tissue engineering for many different applications because they differentiate into multiple cell types depending on their environment. Thin cell sheets of hMSCs could be used to biofabricate 3D tissues to regenerate damaged tissues. During hMSC sheet preparation, the cells are grown on a polydimethylsiloxane (PDMS) substrate. Collagen I is used to coat the PDMS, to improve the cell adhesion. Conventional adsorption methods result in an incomplete coating on PDMS, leading to non-uniform adhesion. This experiment sought to develop a covalent binding method to improve the cell sheet characteristics.

Materials and Methods:

The PDMS substrate used to culture hMSCs was separated into four groups with different surface treatments. The first was untreated, smooth PDMS to act as a control group. The second group was plasma treated on the surface, while the third and fourth both had collagen surface coatings using two different binding methods. One used simple adsorption, where a collagen I solution was allowed to adsorb for 2 hours, and the other used APTES and glutaraldehyde to covalently bind collagen 1 to the surface of the PDMS. hMSCs suspended in alpha-MEM medium were seeded onto the samples and allowed to incubate for 3, 7, and 14 days. Immunofluorescent microscopy was used to determine cell sheet coverage and thickness using rhodamine phalloidin and DAPI staining. Surface roughness and hydrophobicity was characterized using atomic force microscopy, and static sessile drop testing. UV-vis testing was used to confirm the presence of collagen 1 on the surface of the PDMS. In order to determine the DNA and gene concentrations of the cells present, DNA assays and RT-PCR's were performed.

Results and Discussion:

Microscopic imaging of the samples revealed a clear increase in cell density and coverage in the covalent binding samples as opposed to the adsorption samples with an area coverage of 23.4% as compared to 16.1% in adsorption samples. AFM showed that the covalent binding group also had the highest roughness relative to the other groups, more than double the roughness of the adsorption sample. The control sample had the highest contact angle at 102.25 degrees, and the plasma treated sample had the lowest at 32.33 degrees. The covalently bonded sample's contact angle was slightly higher than the adsorption sample at 85.6% and 66.7% respectively. In UV-vis testing, the covalent binding sample showed the highest levels of absorption at 275 nm, followed by adsorption. DNA assays showed that both covalent and adsorption samples increased at similar rates, however, between the 7th and 14th day the adsorption sample DNA levels decreased, while the covalent binding samples continued to increase. Based on the results, it appears that covalently binding the collagen I to the PDMS successfully increased the collagen presence on the surface causing an increased cell density, coverage, and stemness in the resulting cell sheet.

33. Modeling Biocorrosion of Zinc Alloys in Endovascular Environment

Student Presenter: Philip Staublin, Materials Science and Engineering
Faculty Advisor: Dr. Jaroslaw Drelich, Materials Science and Engineering

Introduction:

Zinc has shown promise as a material for biodegradable implanted medical devices. The Surface Innovations research team at Michigan Tech has explored the application of zinc to biodegradable metallic stents. For enhanced control over the bio-absorption rate of zinc stents in the arterial environment, a better understanding of the mechanism and kinetics of zinc corrosion is required. This project aims to quantify major factors which influence biocorrosion of zinc, to allow more precise tuning of zinc corrosion rates through varying alloy composition and surface treatment. To this end, a model of zinc biocorrosion in terms of transport kinetics is developed.

Materials and Methods:

Extensive literature review was conducted to survey existing models of zinc corrosion behavior and evaluate their applicability to biocorrosion in the arterial environment. Data acquired in previous animal studies of zinc biocorrosion were compared to results offered by various models in order to evaluate the models' accuracy. Electrochemical data, including polarization curves and electrical impedance spectroscopic studies, were used to determine the possible rate-determining steps of corrosion.
The parabolic rate model traditionally used to model diffusion controlled oxidation of metals was evaluated, using diffusion data obtained from literature. Adjustments for the conditions in the endovascular environment were estimated. Models considering the diffusion and reaction of hydroxide ions with zinc are also under consideration, as is rate-determining adsorption of oxygen on the zinc oxide surface.

Results and Discussion:

Review of electrochemical data revealed a corrosion mechanism most likely under a diffusion controlled cathodic reaction. The oxygen reduction reaction was found to be the primary cathodic reaction. Therefore, oxygen or hydroxide diffusion is likely the rate determining step of corrosion in the arterial environment. The parabolic rate model failed to fit the biocorrosion rates previously observed in animal studies, possibly because it fails to account for progressive decomposition and reformation of the oxide layer hypothesized to occur in bio-absorption. Additionally, the parabolic law does not consider the interactions of other ions, such as the chloride ion. The failure to account for other ion interaction is common among evaluated corrosion models, which must be considered as corrosion products often include chloride salt compounds. Evaluation of existing oxidation models remains underway, but development of a new model accounting for interactions of ions present in the arterial environment holds the most promise for accurately predicting biocorrosion rates.

34. Risk Assessment and Slope Stability Modelling of a Transportation Corridor in Hindu Kush Range

Student Presenter: Valeria Suarez, Geological Engineering
Faculty Advisors: Dr. Thomas Oommen & Dr. Rudiger Escobar-Wolf, Geological and Mining Engineering and Sciences

Introduction:

The Hindu Kush Range have high relief and unstable slopes where extreme weather can cause landslides, avalanches and other natural disasters with little notice. Salang highway is one of the major land transportation routes through the Hindu Kush region, it connects Kabul to the northern regions of Afghanistan. The highway rises to elevations of 3400 m and is vulnerable to unstable slopes and other geohazards.

Materials and Methods:

This project assesses the risk along the highway by integrating slope information from digital elevation models, distance of slope from the road, height of slope, precipitation data, soil types, vegetation information, and local geologic characteristics.

Results and Discussion:

A moderate spatial-resolution risk assessment map of the highway and slope stability models of the areas with greatest risk were elaborated to aide in the preservation of lives, promotion of a healthy economy, and to provide essential information to emergency response managers in the region.

35. Assessment of the Personal Security State of Highly-Trained and Non-Highly-Trained Users

Student Presenter: Trevor Taubitz, Computer Networking and Systems Administration
Faculty Advisor: Yu Cai, Computer Networking and Systems Administration

Introduction:

In information security, understanding end-user behavior is critical to understanding the security posture of an organization as a whole. Much research on the subject has concluded that attacking these end-users is a highly effective attack vector (e.g. with targeted scam, or “phishing,” emails). What this research tries to understand is the relation between the susceptibility to phishing attacks and other personal security habits, as well as the statistical differences of these security habits between highly trained and non-highly trained end-users.

Materials and Methods:

The study is conducted in three phases. First, a survey is sent out to a participant email list asking to conduct a survey of personal security habits. This survey consists of a general self-assessment of personal security habits (e.g. “how often do you click on email links?”), and security understanding (e.g. “what are common indicators of malicious ‘phishing’ email?”). Second, of those students who agree to the study, a selection is chosen from both the highly trained and non-highly trained groups, and a simulation phishing email is sent with a link to a simulated “malicious” website. This website collects information on how many users from each study group (1) click on the link in the email, and (2) how many submit the form presented on the site. Thirdly, a debriefing document and follow-up survey is sent to all the participants who received the simulation phishing email, which asks general questions about their motivations for either falling or not falling victim to the simulated attack.

Results and Discussion:

Due to the sensitive nature of user credentials, part of the results of the study includes the development of a web-based application that securely collects aggregate user information without collecting or exposing any personally identifiable data. This software will be open-sourced after the final results are collected.

Please note, a large scale test and collection of data will be accomplished pending IRB and IT approval.

Studying the effectiveness of phishing campaigns against highly trained users will hopefully give us much more insight as to the effectiveness of current end user awareness training, and allow us to determine whether this is still a reasonably viable attack vector. This has the potential to further enhance the fields of security training and awareness by understanding the strengths and weaknesses associated with these end user awareness programs. Additionally, it has the potential to give visibility into the personal security habits of the students at Michigan Tech, which can then be used to enhance the Michigan Tech security program.

DeVlieg Foundation

36. Substrate Active Cooling for Weld Based 3D Printing

Student Presenter: Brendan Treanore, Materials Science and Engineering
Faculty Advisor: Dr. Paul Sanders, Materials Science and Engineering

Introduction:

Ongoing work in additive manufacturing is centered on improving printing and material technologies. Currently, plastics in 3D printing is the most ubiquitous. Research in metal 3D printing is focused on making it a feasible manufacturing process. 3D metal printing machines can cost 10's of thousands of dollars and take days to complete prints. What they have in accuracy and potential they give up in printing time, cost, and availability. Michigan Tech's welding based open-source metal 3D printer uses widely available parts at a much lower price to enable metal 3D printing to be more common and affordable.

Materials and Methods:

An actively cooled printing surface is a possible solution to the massive heat throughput in weld based of weld based metal 3D printing. The focus of this research is to begin to understand the effects and possible benefits of using actively cooled substrates for metal 3D printing. The effects this has on printing time, print accuracy, and material properties will be assessed by analyzing and comparing standardized print geometries with and without active cooling.

Results and Discussion:

The analysis showed that the use of a chill plate was beneficial to many printing scenarios. It was possible to shorten the pause time between layers by using the chill plate to increase heat extraction. This allowed for faster overall printing. No significant differences were observed between the standardized prints and those done on the chill plate. This has the potential to greatly shorten the overall print times of large prints that have extreme heat extraction issues. While this is promising for the lower layers, as the layer number increased the heat extraction became less effective and may be less useful for larger and taller prints.

37. The Role of the Genetic Toolkit in the Evolution of Complex Color Patterns of Drosophila Guttifera

Student Presenter: David Trine, Biochemistry and Molecular Biology Concentration; Biology
Faculty Advisor: Thomas Werner, Department of Biological Sciences

Introduction:

We investigated the pigment pattern of Drosophila guttifera to understand how developmental genes regulate multiple target genes in identical expression patterns. D. guttifera displays an array of melanin spots and shades on its wings and body. Our current research focus is on the abdominal pigment pattern of the same species, which consists of six longitudinal spot rows and a dorsal midline shade. The tan (t) and yellow (y) genes are expressed in identical patterns in the abdominal pigment pattern. There are human cancer genes that also show patterns co-expression. Determining the mechanisms responsible will improve our understanding of cancer.

Materials and Methods:

The location of the t gene enhancers driving color pattern expression on developing D. guttifera abdomen was found by dividing the non-coding segments of the t locus into partially overlapping fragments of sizes ranging between 500bp and 5000bp. The t gene fragments were then cloned in front of the red-fluorescent protein (DsRed) gene and placed inside of the piggyBac(pBac) transposon vector. To produce transgenic lines, I worked with graduate student Komal Raja to inject each reporter construct into at least 1000 D. guttifera embryos. Larvae were then screened to find transgenics using a fluorescent microscope. Those having fluorescent-green eye disks when viewed were saved and used to establish transgenic lines. Once the transgenic larvae formed pupae, they were screened for DsRed expression patterns located on their developing abdominal epidermis. DsRed pattern expression was observed on the developing abdominal epidermis when the injected reporter construct contained an enhancer. After identifying an enhancer, the enhancer containing DNA construct was sub-divided into pieces with the help of Komal Raja. This process was then repeated using these pieces.

Results and Discussion:

We identified fragments within t locus which drive DsRed in a pattern that closely resembles the adult abdominal spot pattern. There were three sections of the tan gene locus that each drove expression of a part of the abdominal spot pattern. One regulates full body expression, one shows the entire spot pattern, and a fragment of the spot pattern section showed horizontal stripes when expressed. This could signify that the spots arose from the evolution of a repressor that affects the stripe pattern on the abdomen. Further characterization of t and y abdominal spot enhancers will allow us for the first time, to understand how developmental genes collectively regulate the co-expression of two independent genetic loci.

38. Synthesis and Characterization of Novel Photoactive Lanthanide Complexes

Student Presenter: Randall Wilharm, Chemistry
Faculty Advisor: Dr. Rudy Luck, Chemistry

Introduction:

Catalysts are extremely important to many industrial and research chemical reactions because of their ability to open new reaction pathways and decrease the energy needed for the reactions. The goal of this research is to use the unique photochemical properties of three lanthanide metals, samarium, europium, and terbium, with a novel photoactive ligand to create a new catalyst that harnesses light to push reactions.

Materials and Methods:

The ligand used in the three complexes were synthesized in our lab from a procedure created from work done previously in the lab. The complexes were first characterized with X-Ray crystallography to determine the structure of the complex and the bond distances between the ligand and the metal center. The complexes were then analyzed using TGA to determine the purity of the product and to determine how the complexes decomposed. The IR spectra of the complexes were taken to determine the stretching frequencies found in the complex's bonds. And lastly, the UV-Vis and Fluorescence spectra were taken of the three complexes. This determined the spectroscopic properties of the complexes, informing us of how each complex absorbs light and transfers its energy.

Results and Discussion:

From the X-Ray crystallographic data, the geometry of each complex was determined and the predicted chemical formula, MCl¬3(PN)2 (M = Sm, Eu, Tb; PN = the novel ligand, C22H19N2PO), was confirmed. Additionally, the bond distances between the ligand and the metal were determined and showed the ligand was bonded relatively strongly to the metal. The IR spectra of the complexes compared closely to spectra of the ligand alone, except shifts in the bonds adjacent to the metal-ligand bonds, as expected. The TGA showed that the ligand dissociated from the metal first, before the chlorines, backing up the bond distances measured by the X-Ray crystallographic data. The UV-Vis absorption spectra showed that the complexes absorbed light at the same wavelengths as the ligand by itself, suggesting light is mainly absorbed by the ligand. The Fluorescence spectra of the complexes, however, showed a significant difference to the ligand alone. The emission peaks were shifted to much higher wavelengths, suggesting that the ligand transferred the energy of the absorbed photons to the metal center before the light was re-emitted. This transfer of energy may be able to be used to catalyze other reactions in novel ways.